Geologia Sudetica, 1999, 32: 83–111.

Volcanism in a late Variscan intramontane trough: the petrology and geochemistry of the Carboniferous and Permian volcanic rocks of the Intra-Sudetic Basin, SW Poland

Marek Awdankiewicz

Uniwersytet Wrocławski, Instytut Nauk Geologicznych, Zakład Mineralogii i Petrologii, ul. Cybulskiego 30, 50-204 Wrocław, Poland; e-mail: mawdan@ing.uni.wroc.pl

Key words: Intra-Sudetic Basin, Carboniferous, Permian, late- to post-collisional volcanism, geochemistry, petrology.

Abstract The Carbonifeorus–Permian volcanic rocks of the Intra-Sudetic Basin represent products of late- to post-collisional volcanism associated with extension within the eastern part of the Variscan belt of Europe. The volcanic succession is subdivided into the older, calc-alkaline suite (the early and late Carboniferous) and the younger, mildly alkaline suite (the late Carboniferous and early Permian). The rhyodacites with subordinate basaltic andesites and andesites of the older suite show convergent plate margin affinities. The rhyolitic tuffs, rhyolites with less widespread trachyandesites and basaltic trachyandesites of the younger suite are largely characterised by within-plate affinities, with some gradations towards convergent plate margin affinities. This geochemical variation compares well with that found in some Tertiary–Recent extensional settings adjacent to former active continental margins (e.g. the Basin and Range province of the SW USA). The parental magmas for each suite of the Intra-Sudetic Basin possibly originated from similar, garnet free mantle sources at relatively shallow depths (within the subcontinental mantle?), but at variable degrees of partial melting (lower for the mildly alkaline rocks). The convergent plate margin-like geochemical signatures of the volcanic rocks may either have been inherited from their mantle sources, or be related to the assimilation of crustal rocks by the ascending and fractionating primary magmas. The intermediate-acidic rocks within each suite mainly originated due to fractional crystallisation of variable mineral assemblages equivalent to the observed phenocrysts (mainly plagioclase and pyroxenes, with hornblende and biotite in the calc-alkaline suite, and K-feldspar in the mildly alkaline suite). The trace element patterns of the volcanic rocks were also strongly influenced by fractionation of accessory minerals, such as spinels, ilmenite, zircon, apatite and others. The petrographic evidence (e.g. quartz phenocrysts with reaction rims, complexly zoned or sieve-textured feldspar phenocrysts) suggests that assimilation and/or magma mixing processes might also have taken place during the evolution of the magmas.

Manuscript received 30 November, 1999, accepted 30 December 1999.

INTRODUCTION

The Intra-Sudetic Basin, situated at the NE margin of the Bohemian Massif, represents one of the largest late Palaeozoic intramontane troughs of the eastern part of the European Variscides (Fig. 1). The molasse sequence of the basin provides a well preserved record of the climactic Permo-Carboniferous volcanic phase that affected large areas of late Palaeozoic Europe (e.g. Lorenz & Nicholls, 1976, 1984; Benek *et al.*, 1996). Recent studies in the northern part of the Intra-Sudetic Basin, where the most complete volcanic succession of the area is found, provided new evidence on the location of the volcanic centres, styles of their activity and emplacement sequence of the volcanic rocks (Awdankiewicz, 1999). These results form the geological background for the geochemical and petrological studies reported in the this paper, in which the following problems are particularly addressed:

- the petrography and mineral chemistry of the volcanic rocks,
- the major and trace element geochemistry of the volcanic rocks, and
- the origin of the volcanic rocks, including the magma sources, differentiation mechanisms of the volcanic suites and the palaeotectonic significance of the geochemical variation of the volcanic rocks.

The study was based on chemical analyses of 105 samples of the volcanic rocks by the XRF method, examina-

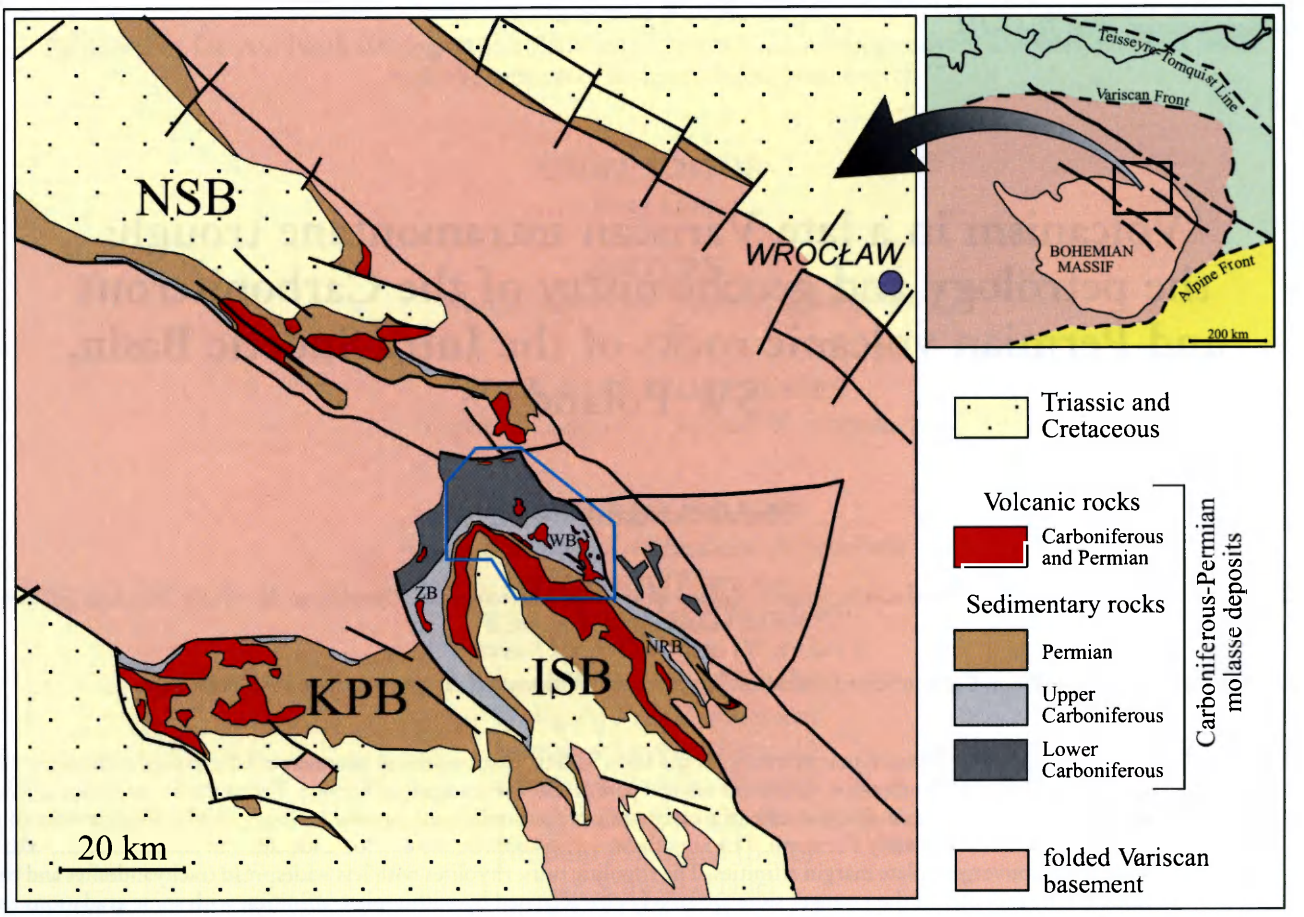

Fig. 1. Distribution of the late Palaeozoic intramontane troughs and molasse deposits in the Sudetes. The study area is marked by the blue box. NSB – North-Sudetic Basin, KPB – Krkonoše Piedmont Basin, ISB – Intra-Sudetic Basin (WB – Wałbrzych Basin, ZB – Žacléř Basin, NRB – Nowa Ruda Basin). The inset shows the area of the main map within the Variscan belt.

tion of ca. 250 thin sections and over 500 chemical analyses of minerals in 34 thin sections with an electron microprobe. Details of the analytical methods are given in the chapters on mineral chemistry and geochemistry. A complete set of rock analyses and ca. 300 mineral analyses, together with detailed sample locations, is contained in Awdankiewicz (1997 b). In this paper representative analyses of minerals (61) and rocks (30) are shown in Tables 1 to 7 and sample locations are marked in Figure 2.

VOLCANIC CENTRES, THEIR EVOLUTION AND VOLCANIC ROCK SUITES

The geology of the Carboniferous–Permian volcanic succession of the northern part of the Intra-Sudetic Basin, including subdivision and correlation of the volcanic rocks, was extensively characterised in Awdankiewicz (1999). In this chapter the key conclusions are briefly outlined, and the two major suites of the volcanic rocks are defined.

The volcanic succession of the northern part of the Intra-Sudetic Basin consists of three volcanic complexes: 1) the lower Carboniferous volcanic complex (the latest Tournaisian/earliest Visean), 2) the upper Carboniferous volcanic complex (the late Westphalian–Stephanian), and 3) the lower Permian volcanic complex (the early Permian), this last corresponding to the climax of volcanic activity. Several volcanic centres, and their successive eruptive products, were distinguished within the complexes (Fig. 2). The evolution of the volcanoes, including the location of the eruption sites and the emplacement mechanisms and the sequence of the volcanic rocks, was reconstructed.

The earliest volcanism occurred near the northern margin of the Intra-Sudetic Basin and the successive volcanoes shifted SE-wards with time, consistently with the intrabasinal depositional centres. The location of the main volcanic centres was controlled by NNW–SSE to NW–SE aligned fault zones within the basin basement. Magmas fed along the fault zones intruded thicker accumulations of sedimentary rocks within intrabasinal troughs, and erupted through thinner sequences outside the troughs. Effusive to extrusive activity created lava-dominated, composite volcanic centres to the north and west, while in the eastern part of the basin the most evolved acidic mag-

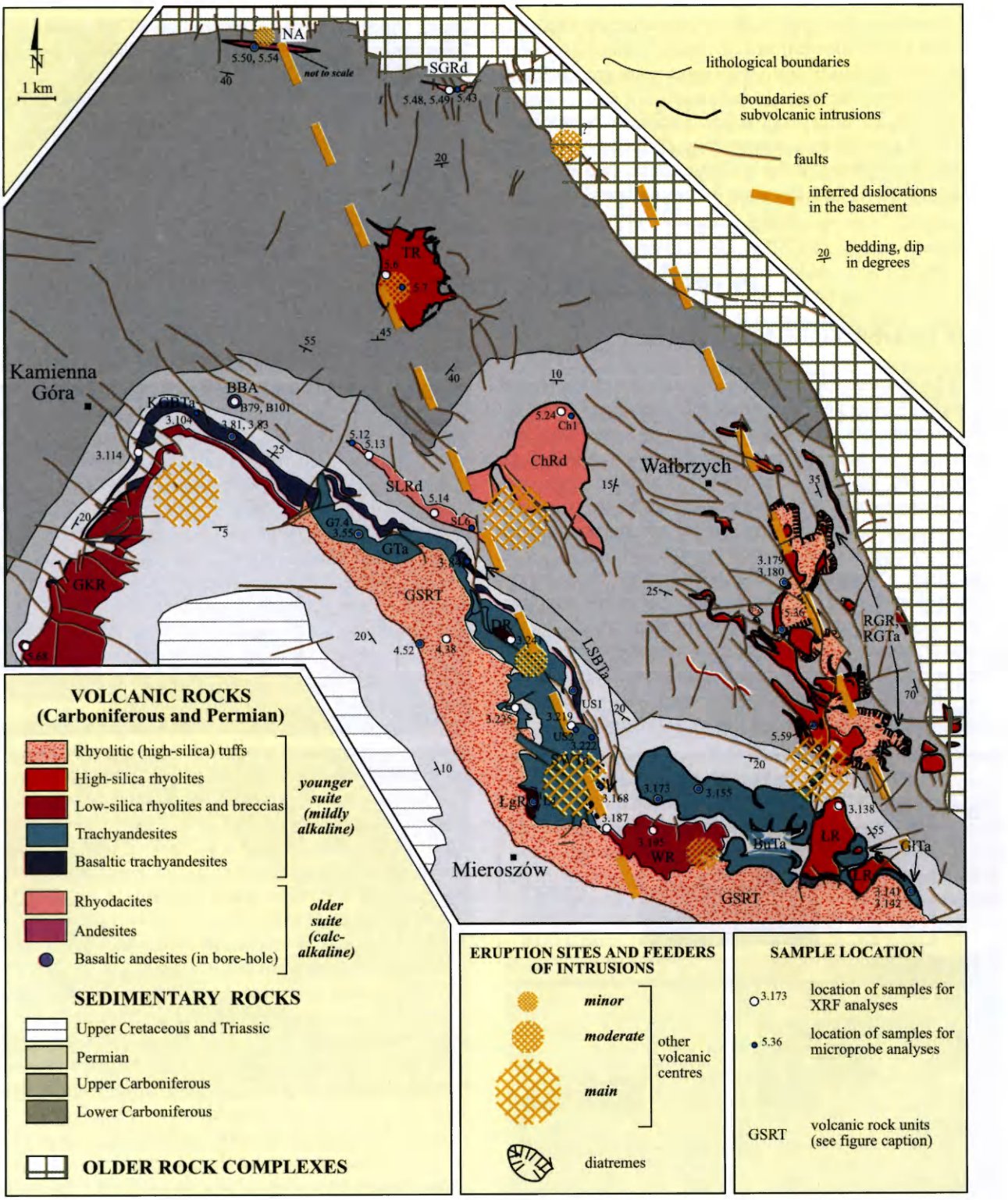

Fig. 2. Geological sketch of the study area showing the distribution of the volcanic rocks, their geological forms, possible eruption sites and their relationship to inferred dislocations in the basement. The locations of samples for the chemical analyses contained in Tables 1 to 7 are indicated. Volcanic rocks units: Lower Carboniferous volcanic complex: SGRd – Sady Górne rhyodacites, NA – Nagórnik andesites. Upper Carboniferous volcanic complex: western Walbrzych Basin volcanic association (BBA – Borówno basaltic andesites, ChRd – Chelmiec rhyodacites, SLRd – Stary Lesieniec rhyodacites, TR – Trójgarb rhyolites), eastern Walbrzych Basin volcanic association (RGTa – Rusinowa–Grzmiąca trachyandesites, RGR – Rusinowa–Grzmiąca rhyolites). Lower Permian volcanic complex: Góry Krucze volcanic association (KGBTa – Kamienna Góra basaltic trachyandesites, GKR – Góry Krucze rhyolites), Unislaw Śląski volcanic association (LSBTa – Lesieniec–Sokolowsko basaltic trachyandesites, SWTa – Stożek Wielki trachyandesites, GTa – Grzędy trachyandesites, DR – Dzikowiec rhyolites, ŁgR – Ługowina rhyolites, WR – Waligóra rhyolites), Rybnica Leśna volcanic association (BuTa – Bukowiec trachyandesites, GlTa – Gluszyca trachyandesites, LR – Łomnica rhyolites), GSRT – Góry Suche rhyolitic tuffs (based on Awdankiewicz, 1999).

mas erupted explosively, with the formation of: 1) a maar belt (late Carboniferous) and 2) a major caldera (early Permian, SE of the study area), with subsequent emplacement of subvolcanic intrusions in both cases.

Specific assemblages of volcanic rocks were emplaced at each of the volcanic centres (Fig. 2). Based on the emplacement sequence of the volcanic rocks, two suites are distinguished: 1) the older suite (early and late Carboniferous), which consists of basaltic andesites, andesites and rhyodacites, and 2) the younger suite (late Carboniferous and early Permian), which consists of basaltic trachyandesites, trachyandesites, rhyolites and rhyolitic tuffs. The suites differ in their petrographic, mineralogical and geochemical characteristics, which are discussed in the following chapters.

PETROGRAPHY OF THE VOLCANIC ROCKS

THE OLDER VOLCANIC SUITE

The volcanic rocks of the older suite are characterised by well developed porphyrytic structures (Fig. 4, 5 and 6). The phenocrysts are usually less than 2–3 mm long, and the largest phenocrysts, typical of the andesites and some rhyodacites, are up to 10 mm in size. The phenocryst content of the basaltic andesites and the andesites is usually less than 10%, and the rhyodacites are represented by phenocryst-poor and phenocryst-rich lithologies, with less than 5%, and 10–50% phenocrysts, respectively (Awdankiewicz, 1999). The phenocrysts of the rhyodacites often form glomeroporphyritic clots which, in the phenocryst-rich lithology, grade into small enclaves (< 10 mm in size) composed of tens to hundreds of crystals.

The variation of phenocryst assemblages in the volcanic rocks is summarised in Figure 3. Phenocrysts of plagioclase (strongly replaced by albite, calcite and kaolinite) and quartz occur throughout the suite, but they are most abundant in the more evolved rock types. Phenocrysts of ferromagnesian minerals (except for biotite) are completely replaced by chlorites, carbonates and opaque minerals, but the characteristic habit, structure and composition of the pseudomorphs enable a general identification of the likely primary mineral phases. Pseudomorphs after pyroxenes (Fig. 5) are found throughout the suite, pseudomorphs after olivine (Fig. 4 a) are characteristic of the basaltic andesites, and pseudomorphs after hornblende (Fig. 6 b) are common in the rhyodacites. The latter rocks also contain biotite phenocrysts (Fig. 6 c). The accessory microphenocrysts comprise apatite, zircon, spinel and ilmenite, the latter two usually found as inclusions in mafic pseudomorphs.

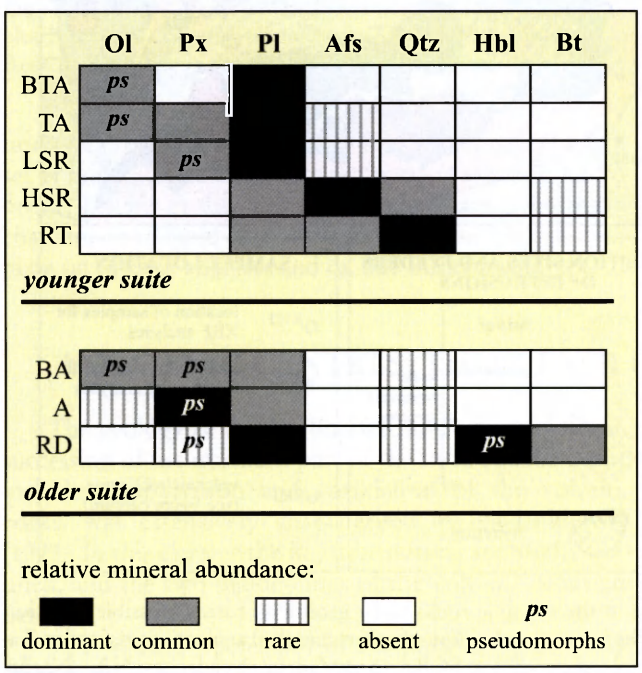

Fig. 3. Major phenocryst assemblages of the volcanic rocks of the Intra-Sudetic Basin. Ol – olivine, Px – pyroxene, Pl – plagioclase, Afs – alkali feldspar, Qtz – quartz, Hbl – hornblende, Bt – biotite. Older volcanic suite: BA – basaltic andesite, A – andesite, RD – rhyodacite. Younger volcanic suite: BTA – basaltic trachyandesite, TA – trachyandesite, LSR – low-silica rhyolite, HSR – high-silica rhyolite, RT – rhyolitic tuff.

Many of the phenocrysts show complex textures generally resulting from disequilibrium growth, partial resorption of the crystals and their reaction with magmas. Plagioclase phenocrysts in all the members of the suite are commonly sieve-textured and those in rhyodacites are often rounded (Fig. 4 b and 6 a). Skeletal habit and honeycomb textures are characteristic of pseudomorphs after pyroxene in the andesites and rhyodacites. Quartz phenocrysts are rounded and embayed, and surrounded by chlorite-, calcite- and opaque mineral-rich overgrowths in the basaltic andesites and andesites (Fig. 4 c).

The microcrystalline groundmass of the volcanic rocks, with a typical grain size below 0.1 mm, shows variable composition and textures. The groundmass of the basaltic andesites and andesites is composed of albitised plagioclase laths and pseudomorphs after ferromagnesian minerals (similar to those found as phenocrysts), with abundant interstitial chlorites, carbonates, quartz, kaolinite and haematite staining (Fig. 4 and 5). Textures range from massive to trachytic, and samples from the marginal parts of igneous bodies show relic hypocrystalline textures, with albite laths scattered in an almost opaque groundmass. The groundmass of the rhyodacites consists of quartz, plagioclase, alkali feldspars and variable amounts of carbonates, chlorites, kaolinite and haematite (Fig. 6). Poikilomosaic and felsitic textures are characteristic of the intrusions, while felsitic and trachytic textures are typical of the lavas. Flow banding, defined by grain-size variation and haematite staining, is well developed in places.

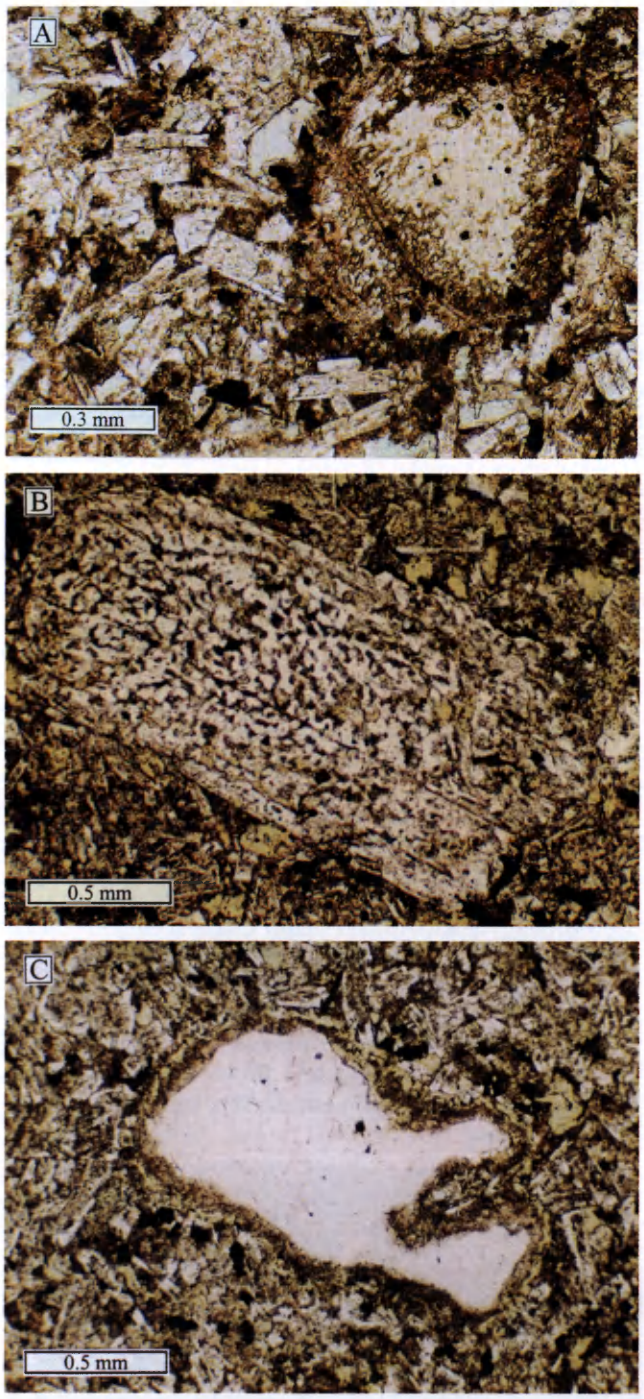

Fig. 4. Photomicrographs of the Borówno basaltic andesites (bore hole Borówno 2, Fig. 2). All photos in plane polarised light. **A** – chlorite-calcite pseudomorph after an olivine phenocryst in a sample from a depth of 79.5 m. The intersertal-textured groundmass consists of albitised plagioclase laths, chlorite pseudomorphs after pyroxenes and/or volcanic glass(?) and opaque minerals. **B** – sieve-textured, albitised plagioclase phenocryst in a sample from a depth of 101.75 m. Groundmass texture and composition as above. **C** – corroded and embayed quartz phenocryst with a chlorite-calcite halo in a sample a from depth of 100.5 m. Groundmass texture and composition as above.

THE YOUNGER VOLCANIC SUITE

The volcanic rocks of the younger suite are usually characterised by porphyrytic structures, although almost aphanitic rocks, with sparse and small phenocrysts, are common. The phenocryst content of the basic and intermediate rocks is usually ca. 2–5% or less, occasionally ranging up to 15%, and the phenocrysts are less than 2 mm in size. The rhyolites typically contain less than 15% phenocrysts, which are up to 0.5 mm, and 1–2 mm long, in the low- and high-silica rhyolites, respectively. The highest phenocryst content (ca. 30%) and size (up to 15 mm) are characteristic of some high-silica rhyolites (Ługowina rhyolites).

The petrographic features of the volcanic rocks are illustrated in Figures 7 to 10. The phenocryst assemblages vary systematically from the most primitive to most evolved rock types (Fig. 3). Plagioclase phenocrysts, together with accessory opaque microphenocrysts, occur throughout the suite. They are associated with pseudomorphs after olivine in the basaltic trachyandesites and trachyandesites. The latter also contain pyroxene phenocrysts (often completely replaced by chlorites), both augite and pigeonite, and occasionall alkali feldspar phenocrysts. Plagioclase and alkali feldspar are the dominant phenocrysts of the rhyolites. The low-silica rhyolites also contain abundant pseudomorphs after pyroxenes, while quartz and biotite are characteristic of the high-silica rhyolites. Quartz phenocrysts predominate over feldspars in the rhyolitic tuffs. Rounded and sieve-textured phenocrysts of plagioclase, alkali feldspar and quartz are found in some of the basic and intermediate rocks.

The main groundmass components of the basaltic trachyandesites and trachyandesites are plagioclase, pyroxenes (augite and pigeonite, the latter more common in the trachyandesites) and pseudomorphs after olivine. Both rock types also contain alkali feldspar overgrowths on plagioclase laths, interstitial clay minerals (largely a replace-

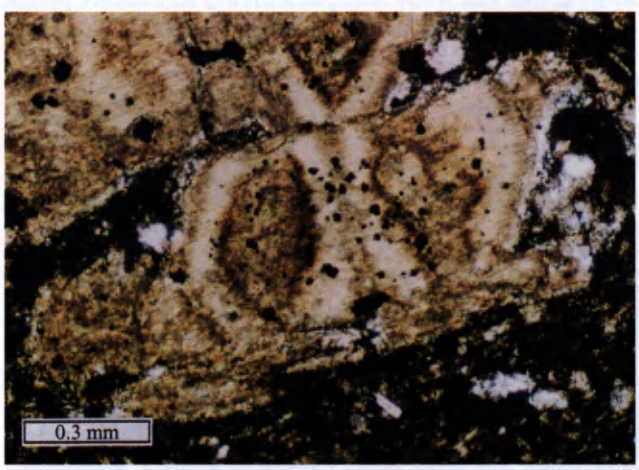

Fig. 5. Photomicrograph of a kaolinite-calcite-dolomite pseudomorph after a pyroxene (?) phenocryst with chromian spinel inclusions in the Nagórnik andesites. The groundmass consists of albitised plagioclase laths with interstitial aggregates of kaolinite, calcite, quartz and chlorite, with abundant haematite staining. Crossed polars.

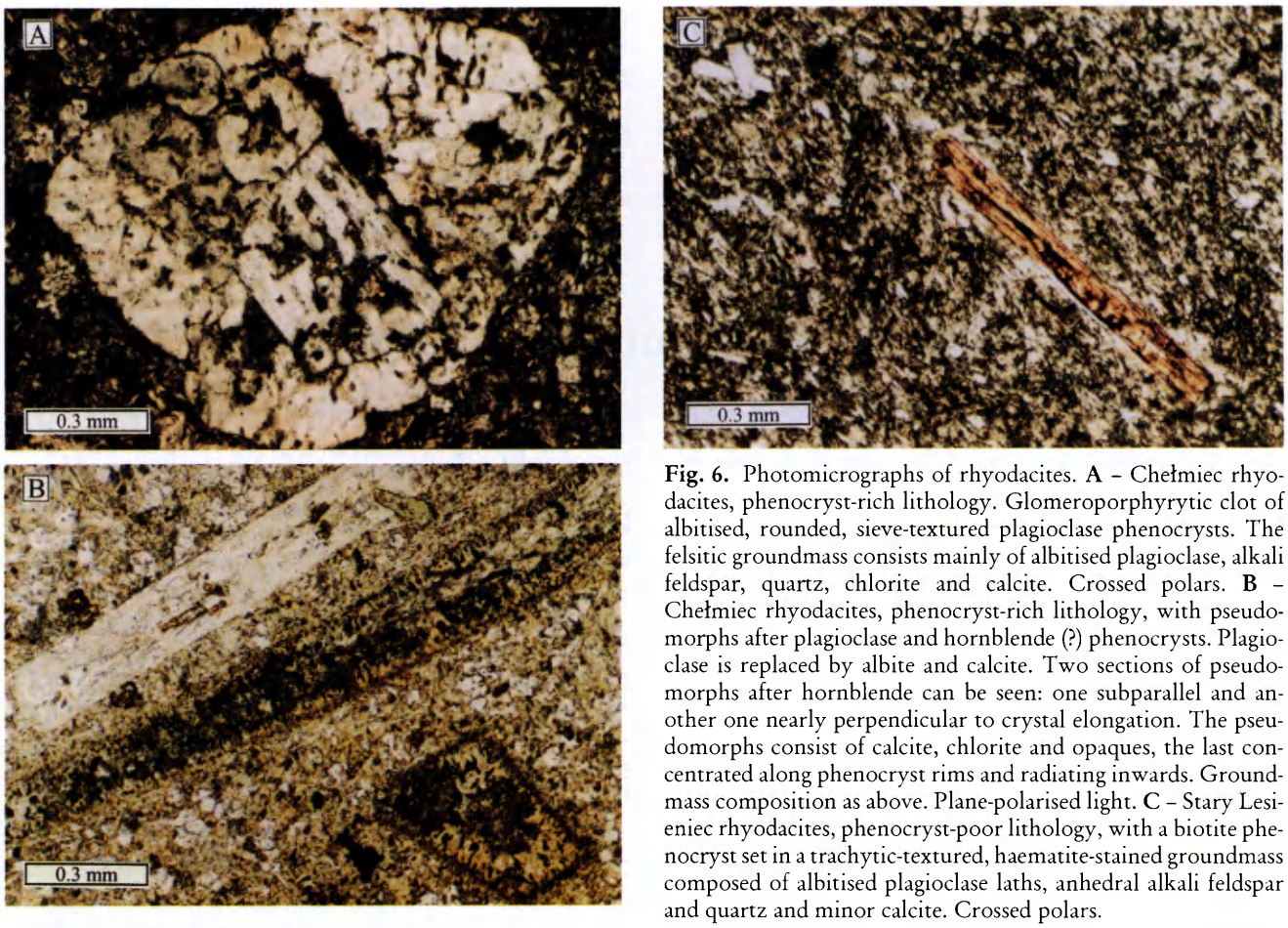

Fig. 6. Photomicrographs of rhyodacites. **A** – Chełmiec rhyodacites, phenocryst-rich lithology. Glomeroporphyrytic clot of albitised, rounded, sieve-textured plagioclase phenocrysts. The felsitic groundmass consists mainly of albitised plagioclase, alkali feldspar, quartz, chlorite and calcite. Crossed polars. **B** – Chełmiec rhyodacites, phenocryst-rich lithology, with pseudomorphs after plagioclase and hornblende (?) phenocrysts. Plagioclase is replaced by albite and calcite. Two sections of pseudomorphs after hornblende can be seen: one subparallel and another one nearly perpendicular to crystal elongation. The pseudomorphs consist of calcite, chlorite and opaques, the last concentrated along phenocryst rims and radiating inwards. Groundmass composition as above. Plane-polarised light. **C** – Stary Lesieniec rhyodacites, phenocryst-poor lithology, with a biotite phenocryst set in a trachytic-textured, haematite-stained groundmass composed of albitised plagioclase laths, anhedral alkali feldspar and quartz and minor calcite. Crossed polars.

ment product of volcanic glass), and accessory opaque minerals and apatite. However, the trachyandesites are distinguishable from the basaltic trachyandesites due to abundant interstitial quartz and, locally (see below), groundmass hornblende and biotite (e.g. Fig. 7 b and 8 a).

The basaltic trachyandesites are petrographically uniform across the study area, although a significant petrographic variation is observed in well exposed vertical sections of several igneous bodies. Overall, holocrystalline, ophitic or intergranular and massive rocks typical of the interiors of igneous bodies grade outwards into hypocrystalline, trachytic-textured, vesicular, strongly altered lavas (Awdankiewicz, 1997 a).

However, much stronger petrographic diversity is typical of the trachyandesites. This diversity reflects both the variable geological forms of these rocks and a wider

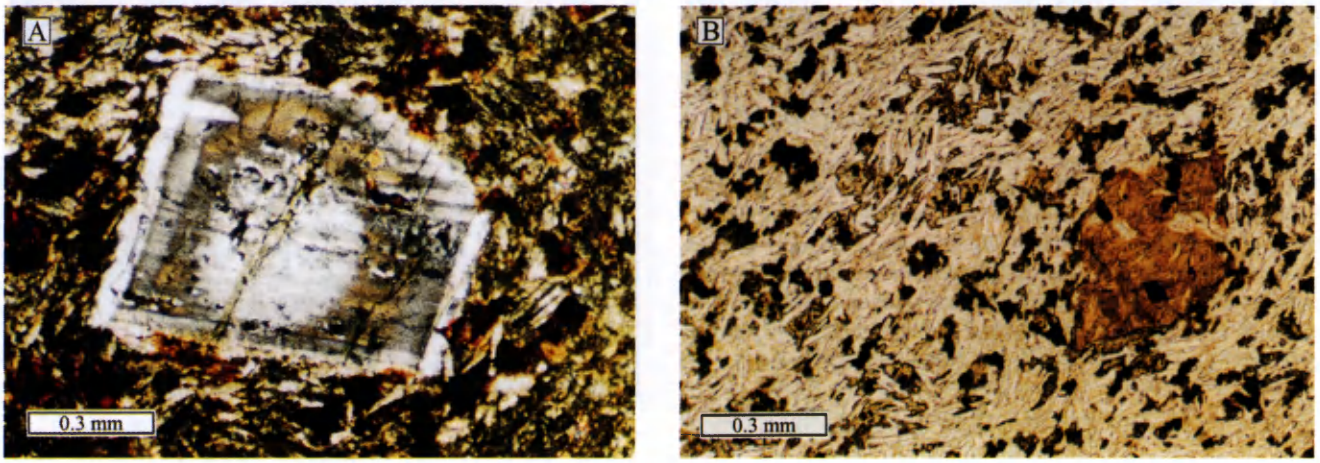

Fig. 7. Photomicrographs of the Kamienna Góra basaltic trachyandesites. **A** – zoned plagioclase phenocryst with a rounded core set in a groundmass of plagioclase laths and abundant opaques. Crossed polars. **B** – smectite pseudomorph after olivine in a groundmass of aligned plagioclase laths (partly overgrown by alkali feldspars), opaque minerals, augite (pale brown, high relief) and interstitial smectites (pale brown, low relief). Plane polarised light.

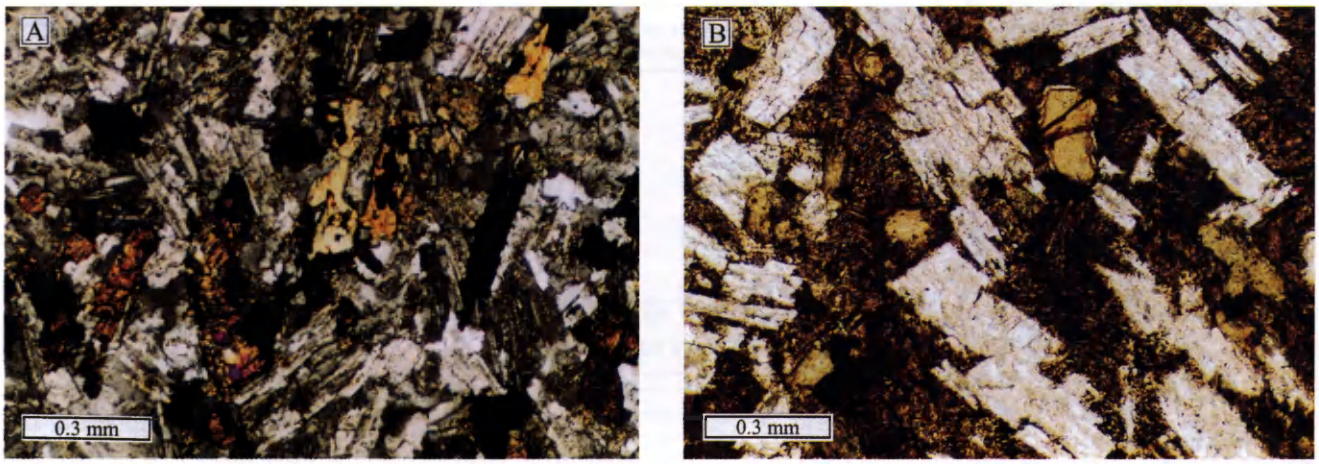

Fig. 8. Photomicrographs of trachyandesites. **A** – fine-grained trachyandesite from the central part of a thick subvolcanic intrusion (Bukowiec trachyandesites). The rock is composed of plagioclase laths, pyroxene prisms (partly replaced by chlorite and opaque minerals) and yellowish-brown hornblende. The interstitial components are quartz and alkali feldspar. Crossed polars. **B** – quench-textured trachyandesite from the marginal part of a subvolcanic intrusion (Łomnica trachyandesites). The rock consists of albitised plagioclase laths, some of which show a skeletal habit, and chlorite pseudomorphs after ferromagnesian minerals, set in haematite-rich groundmass of albite microliths with a fan-shaped arrangement. Plane polarised light.

Fig. 9. Photomicrographs of rhyolites. **A** – pseudomorphs after small pyroxene (?) phenocrysts in a low-silica rhyolite (Waligóra rhyolites). The pseudomorphs are composed of kaolinite and opaque minerals. The felsitic groundmass consists of anhedral alkali feldspars, quartz and clay minerals. Plane polarised light. **B** – alkali feldspar phenocryst (anorthoclase) in a high silica rhyolite (Rusinowa–Grzmiąca rhyolites). The felsitic groundmass is composed of anhedral quartz and alkali feldspar and is rich in haematite staining. Crossed polars. **C** – quartz, alkali feldspar and albitised plagioclase phenocrysts in a high-silica rhyolite (Łomnica rhyolites). Groundmass texture and composition similar to above.

range of chemical compositions, compared with the basaltic trachyandesites. The trachyandesites of the central parts of thick intrusive bodies (the Bukowiec and Głuszyca trachyandesites) are relatively coarse-grained (phaneritic), intergranular- and massive textured rocks, with hornblende and biotite found as isolated groundmass crystals and overgrowths on pyroxene prisms (Fig. 8 a). Some of the pyroxenes show poorly developed exsolution lamellae. Outwards, a gradation into variably developed, hypocrystalline, quench-textured and strongly altered rocks is observed (Fig. 8 b). The trachyandesites of the lava flows (Grzędy trachyandesites), domes (Stożek

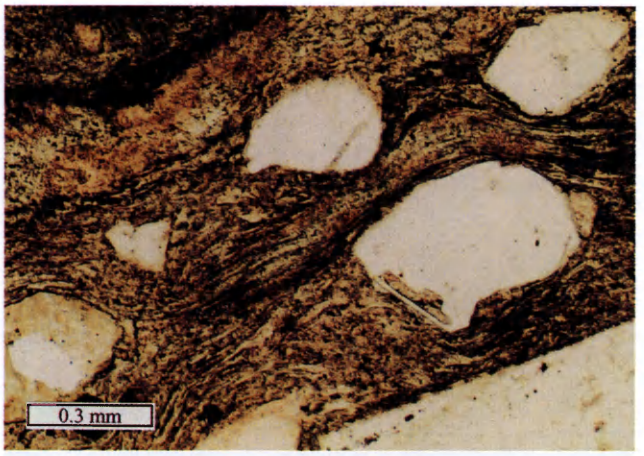

Fig. 10. Photomicrograph of a strongly welded tuff with eutaxitic texture (Góry Suche rhyolitic tuffs, uppermost part of an ignimbrite sheet). Aligned glass shards and pumice, recrystallized into alkali feldspar and quartz, are squeezed between quartz and feldspar phenocrysts. Plane polarised light.

Wielki trachyandesites) and small intrusions (Rusinowa–Grzmiąca trachyandesites) compare well petrographically with the outer to marginal parts of the thick intrusions: they are relatively fine-grained (aphanitic), hornblende and biotite are not present, and olivine and pyroxenes are almost completely replaced with secondary minerals. In addition, the chemically more evolved Stożek Wielki trachyandesites (relatively rich in silica and alkalis) are also distinguished by their greater quartz and alkali feldspar contents (Awdankiewicz, 1997 b).

Similarly to the trachyandesites, the rhyolites also show a significant petrographic variation. These rocks comprise high- and low-silica types (see the chapter on geochemistry) and form lavas, domes, small intrusions and pyroclastic rocks of various origin (Awdankiewicz, 1999). The groundmass of the rhyolites is mainly composed of alkali feldspars and quartz with abundant haematite staining. Felsitic textures are most typical (Fig. 9), but trachytic and poikilomosaic textures are also characteristic of the low-silica rhyolites, while spherulitic and poikilomosaic textures are observed in the high-silica rhyolites. The latter are often flow-banded and consist of texturally variable laminae and aligned quartz, calcite or kaolinite streaks. A specific variety of the high-silica rhyolites are spheroidal rhyolites which contain abundant, concentrically laminated structures up to 20–30 cm in diameter (Awdankiewicz, 1997 b).

The rhyolitic tuffs represent pyroclastic equivalents of the high-silica rhyolites. The main components of the tuffs are devitrified, recrystallized glass shards (replaced by quartz, clay minerals, carbonates and haemetite), with variable amounts of pumice, crystals, rhyolite clasts and accretionary lapilli. Some of these rocks (e.g. those of the Rusinowa–Grzmiąca rhyolite unit, and the bedded tuffs of the Góry Suche rhyolitic tuffs unit, Awdankiewicz, 1999) grade towards tuffites and contain significant amounts of lithic clasts (gneisses, mica schists, quartzites, phyllites, trachyandesites, mudstones and others) and accessory minerals (white mica, garnet, sphene) probably derived from the basement and country rocks on eruption.

A systematic petrographic variation is observed in vertical section of the ignimbrite sheet forming the main part of the Góry Suche rhyolitic tuffs. This ignimbrite sheet is partly eroded and consists of a nonwelded lower part and a welded upper part (Awdankiewicz, 1999). With the increasing degree of welding, the texture of the tuff grades from chaotic to eutaxitic (Fig. 10). Glass shards in the nonwelded tuffs are replaced by fine-grained quartz or, more rarely, by clay minerals and calcite. At the transition from nonwelded to welded tuffs replacement of the glass shards by an almost cryptocrystalline chalcedony is characteristic. Shards and pumice in the welded tuffs are replaced by alkali feldspar and quartz, often with well developed axiolitic textures. At various levels within the ignimbrite sheet strong recrystallization obscures the original clastic textures, and some of the welded tuffs show a lava-like appearance, resembling the felsitic rhyolites.

MINERAL CHEMISTRY OF THE VOLCANIC ROCKS

ANALYTICAL METHODS

More than 500 analyses of minerals in 34 samples were performed. All the rock types distinguished were analysed in at least one thin section, except for the basaltic andesites which have not yet been analysed. The analyses were largely obtained with the Cambridge Microscan 5 microprobe at the British Geological Survey in Keyworth, United Kingdom (23 thin sections, 70% of the analyses), and also with the Camebax microprobe at Universite Blaise Pascal, Clermont-Ferrand, France (11 thin sections, including 6 analyzed by Prof. R. Kryza). The typical analytical conditions for Cambridge Microscan 5 were: counting time 60 s, beam current 10 nA, accelerating voltage 15 kV, and for Camebax: counting time 10 s, beam current 10 nA, accelerating voltage 15 kV. Representative analyses are shown in Tables 1 to 6, together with calculated mineral formulae and notes on the methods used for the calculations. The sample locations are indicated in Figure 2.

FELDSPARS

Feldspars represent the main mineral component of the volcanic rocks and 342 analyses of feldspars were obtained. The variation of feldspar composition in the volcanic rocks is shown in Figure 11 and selected analyses of feldspar phenocrysts are contained in Tab. 1.

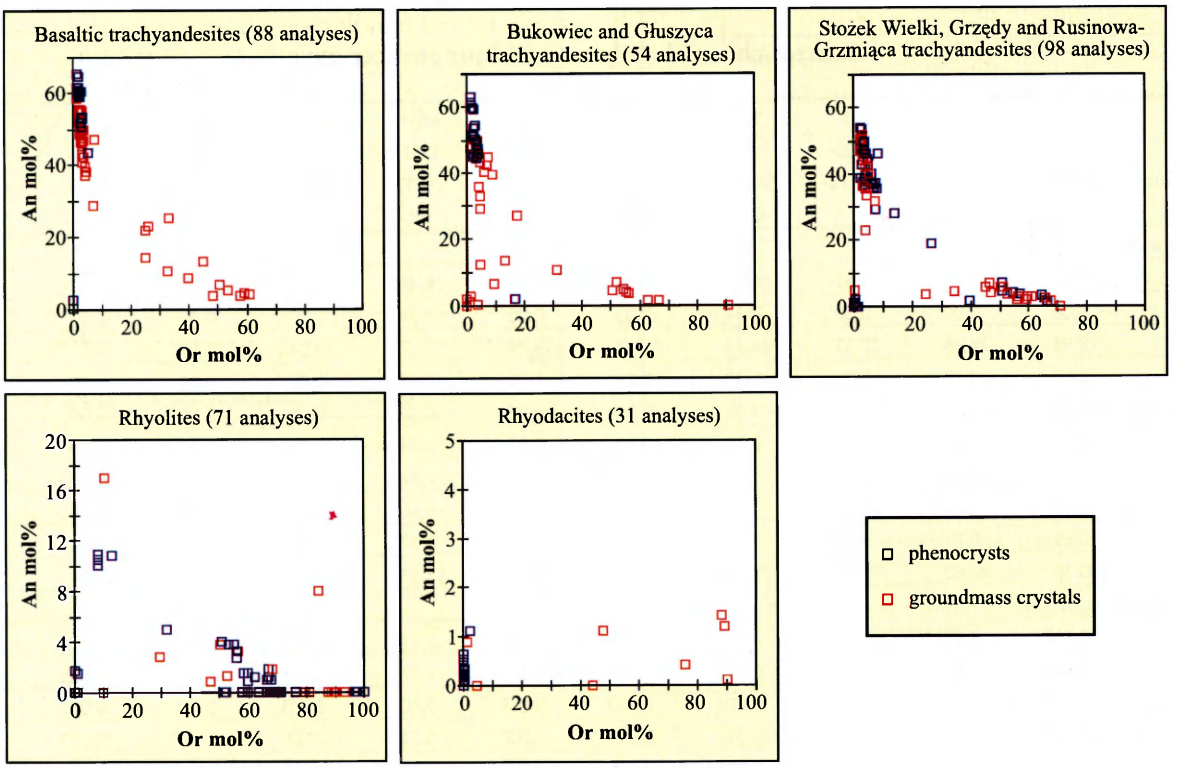

Fig. 11. Variation of feldspar composition in the volcanic rocks.

Plagioclase in the volcanic rocks of the older suite is usually completely replaced by albite and variable amounts of kaolinite and/or calcite. Unaltered plagioclase phenocrysts in the basaltic andesites show oscillatory zoning and an andesine composition (An 45-35, determined by optical methods), while relics of oligoclase/andesine (An 31) were analysed in a rhyodacite sample on the rim of an albitised phenocryst. Alkali feldspar analyses of good quality were only obtained from the rhyodacites. These feldspars contain ca. 40–90% Or and less then 2% An (Fig. 11).

The post-magmatic replacement of the feldspars by albite, kaolinite and carbonates is much less pronounced in the volcanic rocks of the younger suite. Feldspar composition changes consistently with the bulk chemistry of the host rocks (Fig. 11): with silica enrichment of the volcanic rocks, compositional ranges of plagioclase shift towards lower An and higher Or contents, and alkali feldspar ranges shift towards lower An and higher Or contents.

The basaltic trachyandesites contain plagioclase with the highest An contents (up to An65 in phenocryst cores). The phenocrysts are more calcic than groundmass plagioclase laths. Both plagioclase phenocrysts and groundmass crystals usually show weak normal, oscillatory zoning, with a small (< 5%) decrease of An content from core to rim. The strongest normal zoning (up to ca. 25% less An at rim than at core) was observed in groundmass plagioclase laths. Reversely zoned groundmass plagioclase, with up to a 10% An content increase towards crystal rims, is rare. Groundmass alkali feldspars contain between ca. 20 and 60% Or.

The trachyandesites are characterised by a greater diversity of feldspar composition, zoning and textural patterns. Significant differences are observed between the large intrusions (Bukowiec and Głuszyca trachyandesites) and the lava flows, domes and minor intrusive bodies (Grzędy, Stożek Wielki and Rusinowa–Grzmiąca trachyandesites, Figure 11). The plagioclase compositional variation in the large intrusions is similar to that found in the basaltic trachyandesites (relatively calcic phenocrysts with up to An63 in the cores, less calcic groundmass laths, usually weak normal zoning). However, many plagioclase phenocrysts contain rounded cores and reverse zoning is more common. The groundmass alkali feldspars are more variable than in the basaltic trachyandesites and contain up to ca. 90% Or.

The trachyandesites of the second group contain less calcic plagioclase phenocrysts (up to An55), usually with weak normal zoning. No compositional difference is observed between the plagioclase phenocrysts and groundmass laths. However, feldspar phenocrysts with complex textures and zoning patterns are often observed, including: 1) sieve-textured phenocrysts composed of andesine intergrown with alkali feldspar, and 2) variably zoned Ab-rich feldspars (e.g. with Or40Ab58 in the core and An39Ab59 at the rim, or with Or27Ab54 in the core and An28Ab58 at the rim). The groundmass alkali feldspars contain up to 70% Or.

The rhyolites contain Ab and Or-rich feldspars, both as phenocrysts and groundmass crystals (Fig. 11). Zoning has not been observed. Relics of a sodic plagioclase (albite/oligoclase) were analysed in the low-silica rhyolites.

Table 1

Selected chemical analyses of feldspar phenocrysts

analysis	8	526	218	205	206	662*	663*	674*	75	314	355
sample	3.104	3.155	3.222	3.222	3.222	US2	US2	L4	5.59	5.36	4.52
rock unit	KGBTa	BuTa	SWTa	SWTa	SWTa	SWTa	SWTa	ŁgR	RGR	RGR	GSRT
mineral	P	P	P	PC	PR	PC	PR	P	P	P	P
oxides, wt%											
SiO_2	53.61	51.49	54.51	66.25	59.06	66.37	56.46	65.82	66.70	64.90	65.09
TiO_2	0.00	0.00	0.00	0.34	0.00	0.00	0.34	0.00	0.00	0.00	0.00
Al_2O_3	28.98	28.95	27.32	18.34	24.67	19.74	25.27	19.04	20.88	18.45	18.62
Fe_2O_3	0.62	0.72	0.74	0.29	0.75	1.70	0.63	0.29	0.00	0.00	0.33
MnO	0.00	0.00	0.00	0.00	0.00	0.02	0.00	0.19	0.00	0.00	0.00
MgO	0.00	0.00	0.00	0.00	0.00	0.03	0.04	0.02	0.00	0.00	0.00
CaO	13.16	12.37	10.62	0.61	7.34	0.22	7.76	0.66	2.23	0.00	0.00
Na_2O	3.68	3.83	4.77	3.49	6.66	5.64	6.66	5.21	9.13	0.33	3.59
K_2O	0.25	0.24	0.45	10.68	0.56	5.85	0.37	8.82	1.40	16.36	11.46
Total	100.30	97.60	98.41	100.00	99.04	99.58	98.05	100.06	100.34	100.04	99.09
cations per formula unit											
Si	2.430	2.401	2.508	3.005	2.674	2.987	2.598	2.975	2.925	2.998	2.992
Al	1.548	1.591	1.481	0.980	1.316	1.047	1.371	1.014	1.079	1.005	1.009
Fe^{+3}	0.007	0.008	0.009	0.003	0.009	0.019	0.007	0.003	0.000	0.000	0.004
Ti	0.000	0.000	0.000	0.012	0.000	0.000	0.012	0.000	0.000	0.000	0.000
Mn	0.000	0.000	0.000	0.000	0.000	0.001	0.000	0.007	0.000	0.000	0.000
Mg	0.000	0.000	0.000	0.000	0.000	0.002	0.003	0.001	0.000	0.000	0.000
Ca	0.639	0.618	0.523	0.030	0.356	0.011	0.383	0.032	0.105	0.000	0.000
Na	0.323	0.346	0.425	0.307	0.585	0.492	0.594	0.457	0.776	0.03	0.32
K	0.014	0.014	0.026	0.618	0.032	0.336	0.022	0.509	0.078	0.964	0.672
Total	4.961	4.978	4.972	4.955	4.972	4.895	5.01	4.998	4.963	4.997	4.997
end members, mol%											
An	65.47	63.19	53.70	3.14	36.59	1.66	38.52	3.98	10.95	0.00	0.00
Ab	33.09	35.38	43.63	32.15	60.12	58.43	59.28	45.43	80.92	3.02	32.26
Or	1.43	1.43	2.67	64.71	3.29	39.90	2.20	50.60	8.13	96.98	67.74

Number of cations based on 8 O. Total Fe = Fe^{+3}.
Analyses marked with '*' include 0.1–0.5% of Cr_2O_3 and/or NiO.
Rock units: KGBTa – Kamienna Góra basaltic trachyandesites, BuTa – Bukowiec trachyandesites, SWTa – Stożek Wielki trachyandesites, ŁgR – Ługowina rhyolites, RGR – Rusinowa-Grzmiąca rhyolites, GSRT – Góry Suche rhyolitic tuffs.
Minerals: P – phenocryst (C – core, R – rim). End members: An – anorthite, Ab – albite, Or – orthoclase.

Or-rich feldspars (Or50 to Or100), and the highest Or contents in the feldspars, are characteristic of the high-silica rhyolites. The feldspar composition of the rhyolitic tuffs (Góry Suche rhyolitic tuffs) is similar to that of the high-silica rhyolites (Or66-70 in phenocrysts, Or89-93 in groundmass feldspars).

PYROXENES, AMPHIBOLES AND OLIVINE

Due to post magmatic alteration, these minerals are often completely replaced by variable secondary mineral assemblages, with chlorites, carbonates and opaque minerals being most common. However, unaltered pyroxenes, amphiboles and relic olivine are found in the basaltic trachyandesites and some trachyandesites. Representative analyses of these minerals are given in Table 2 and all the pyroxene analyses obtained are plotted in Figure 12.

The basaltic trachyandesites contain groundmass augite and occasional pigeonite. A single poor quality analysis of an olivine relic in a web-textured pseudomorph gave a hortonolite composition (Fo45).

Both augite and pigeonite are found in the Bukowiec trachyandesites. Augite forms phenocrysts and groundmass crystals, while pigeonite mainly occurs in the groundmass. The pyroxenes are accompanied and partly overgrown by amphiboles of edenite composition. A greater compositional variation of pyroxenes and amphiboles is characteristic of the Głuszyca trachyandesites, where augite and edenite are accompanied by ferroaugite, actinolite-hornblende and actinolite (Tab. 2).

On the En-Wo-Fs plot (Fig. 12) pyroxene analyses of the basaltic trachyandesites and the trachyandesites form rather tight clusters. Despite some overlap, a systematic

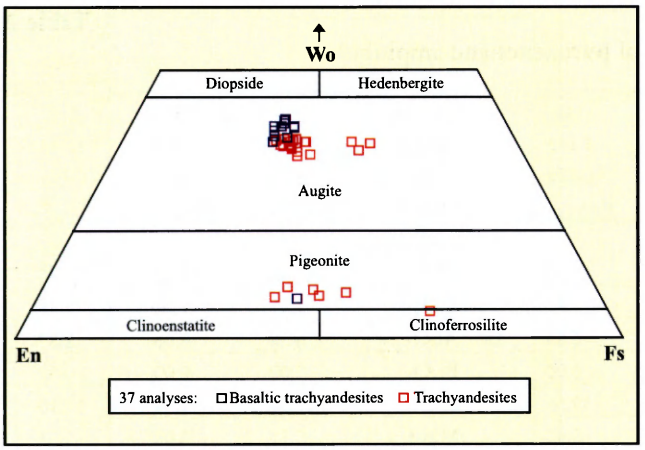

Fig. 12. Variation of pyroxene composition in the basaltic trachyandesites and trachyandesites.

shift in pyroxene composition with the variation in the bulk chemistry of their host rocks is seen: the Fs content of the pyroxenes increases, and Wo content decreases, with silica enrichment of the volcanic rocks.

BIOTITE AND WHITE MICA

Biotite represents the only unaltered primary ferromagnesian silicate in the volcanic rocks of the older suite, where it forms phenocrysts, and more rarely groundmass crystals, in the rhyodacites. In the younger suite biotite is found as: 1) groundmass crystals in intrusive trachyandesites (Bukowiec trachyandesites) and 2) phenocrysts in the high-silica rhyolites (Rusinowa–Grzmiąca and Trójgarb rhyolites, and Góry Suche rhyolitic tuffs). The biotite composition is variable (Fig. 13, Tab. 3), and partly correlates with the bulk chemistry of its host rocks: e.g. the Mg/(Mg+Fe) ratios and Ti contents of the biotites generally decrease with silica enrichment of the volcanic rocks, from trachyandesites through rhyodacites to rhyolites. However, the variation of other chemical components of the biotites is more complex and not well constrained, partly due to the relatively low number of analyses obtained.

Accessory white mica phenocrysts (single plates and glomerocrysts with alkali feldspars and quartz) were encountered in some high-silica rhyolites (Rusinowa–Grzmiąca rhyolites). Four microprobe analyses from two mica plates showed low totals (90–93%). The analysed mica differs from muscovite, having higher Si and lower Al contents, a higher Mg and Fe sum (0.2–0.3 cations per formula unit), and K deficiency (Tab. 3). This mica possibly represents a hydromuscovite.

OPAQUE MINERALS

Opaque minerals represent a widespread minor component of the volcanic rocks. However, many of the opaque grains were found to be mixtures of Fe-Ti oxides and silicates, and good quality microprobe analyses were

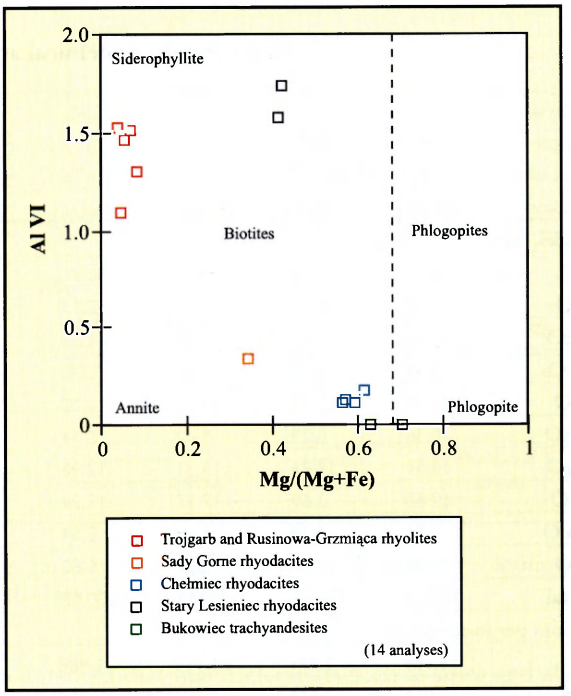

Fig. 13. Variation of biotite composition in the volcanic rocks.

difficult to obtain (low totals). Nevertheless, chromian spinel, magnetite, Ti-magnetite and ilmenite were identified (Tab. 4).

In the older suite chromian spinel is found in the andesites as inclusions in pseudomorphs after pyroxene. Opaque inclusions in various phenocrysts in the rhyodacites were identified as magnetite and ilmenite.

Most of the analysed grains in the volcanic rocks of the younger suite represent Ti-magnetite or ilmenite. Both these minerals are characterised by variable Fe/Ti ratios (Fig. 14). The Ti-magnetite compositions are intermediate between the end-members ulvite and magnetite, while the analysed ilmenites contain less FeO and more TiO_2 than the theoretical composition.

CHLORITES AND CLAY MINERALS

Chlorite is a widespread alteration product of ferromagnesian minerals and volcanic glass in all the volcanic rock types of the Intra-Sudetic Basin. It is also found as vesicle fill in the basic-intermediate lavas. Despite its position in the rock and origin, the chlorite shows a rather weak chemical variation and it is usually of a diabantite composition (Tab. 5, Fig. 15). However, the diabantites from the less evolved rocks (andesites, basaltic trachyandesites) are characterised by a lower Si content than the chlorites of the more evolved rocks (trachyandesites, rhyodacites). Other chlorite compositions encountered include brunsvigite (in a pseudomorph after olivine in a trachyandesite) and talc-chlorite (in the groundmass of a basaltic trachyandesite and rhyolite, and as an alteration product of glass shards in rhyolitic tuffs).

Less altered samples of the basaltic trachyandesites (with fresh pyroxenes and plagioclase present) contain

Table 2

Representative chemical analyses of pyroxenes and amphiboles

analysis	795	719	145	150	528	142
sample	3.84	3.81	3.173	3.173	3.155	3.142
rock unit	LSBTa	KGBTa	BuTa	BuTa	BuTa	GłTa
mineral	Aug, G	Pig, G	Aug, P	Aug, G	Pig, G	FeAug, G
oxides, wt%						
SiO_2	52.14	51.56	53.19	52.72	50.98	51.00
TiO_2	0.62	0.30	0.74	0.73	0.42	0.57
Al_2O_3	0.41	0.33	1.45	1.25	0.49	0.63
Fe_2O_3	1.48	1.15	0.00	0.00	0.00	0.00
FeO	10.78	24.41	13.01	14.00	27.77	19.56
MnO	0.36	0.79	0.42	0.54	0.74	0.42
MgO	14.51	17.75	13.31	12.98	13.69	9.63
CaO	19.53	3.69	17.17	17.24	3.83	16.78
Na_2O	0.16	0.04	0.52	0.54	0.00	0.53
K_2O	0.05	0.04	0.00	0.00	0.00	0.00
Total	100.04	100.06	99.81	100.00	97.92	99.12
cations per formula unit						
Si^{IV}	1.959	1.971	1.994	1.986	2.015	1.993
Al^{IV}	0.018	0.015	0.006	0.014	0.000	0.007
$Fe^{+3\,IV}$	0.023	0.014	0.000	0.000	0.000	0.000
T site	2.000	2.000	2.000	2.000	2.015	2.000
Al^{VI}	0.000	0.000	0.058	0.042	0.023	0.022
Ti	0.018	0.009	0.021	0.021	0.012	0.017
$Fe^{+3\,VI}$	0.019	0.019	0.000	0.000	0.000	0.000
Fe^{+2}	0.339	0.780	0.408	0.441	0.918	0.639
Mn	0.011	0.026	0.013	0.017	0.025	0.014
Mg	0.813	1.011	0.744	0.729	0.807	0.561
Ca	0.786	0.151	0.690	0.696	0.162	0.703
Na	0.012	0.003	0.038	0.039	0.000	0.04
K	0.002	0.002	0.000	0.000	0.000	0.000
M1,M2 sites	2.000	2.001	1.972	1.985	1.947	1.996
end members, mol%						
En	40.83	50.52	40.11	38.72	42.21	29.26
Fs	19.69	41.93	22.70	24.32	49.32	34.06
Wo	39.48	7.55	37.20	36.96	8.47	36.67

analysis	143	257	128
sample	3.142	3.155	3.142
rock unit	GłTa	BuTa	GłTa
mineral	Ed, G	Ed, G	Act, G
oxides, wt%			
SiO_2	47.46	47.82	49.40
TiO_2	1.45	1.42	0.48
$Ał_2O_3$	6.08	5.06	2.82
Fe_2O_3	0.00	0.00	0.00
FeO	17.56	19.24	17.10
MnO	0.31	0.00	0.33
MgO	11.70	10.95	9.72
CaO	10.30	10.10	15.40
Na_2O	2.39	2.30	0.54
K_2O	1.17	0.87	0.36
H_2O	2.01	1.99	1.97
Total	100.43	99.75	98.12
cations per formula unit			
Si^{IV}	7.073	7.201	7.533
Al^{IV}	0.927	0.799	0.467
T site	8.000	8.000	8.000
Al^{VI}	0.141	0.099	0.040
Ti	0.162	0.161	0.055
Mg	2.599	2.458	2.210
Fe^{+2}	2.098	2.282	2.181
Mn	0.000	0.000	0.043
Ca	0.000	0.000	0.472
C site	5.000	5.000	5.000
Fe^{+2}	0.091	0.141	0.000
Mn	0.039	0.000	0.000
Ca	1.645	1.629	2.000
Na	0.226	0.230	0.000
B site	2.000	2.000	2.000
Ca	0.000	0.000	0.044
Na	0.465	0.442	0.160
K	0.222	0.167	0.070
A site	0.687	0.609	0.273

For pyroxenes cation proportions based on 6 oxygen anions and Fe^{+3} calculated assuming cation sum = 4. For amphiboles cation proportions based on 23 O with total cations (without Ca, Na, K) = 13.
Minerals: Aug – augite, FeAug – ferroaugite, Pig – pigeonite, Ed – edenite, Act – actinolite, P – phenocryst, G – groundmass crystal.
Rocks: LSBTa – Lesieniec-Sokolowsko basaltic trachyandesites, KGBTa – Kamienna Góra basaltic trachyandesites, BuTa – Bukowiec trachyandesites, GłTa – Gluszyca trachyandesites.
End members: En – enstatite, Fs – ferrosilite, Wo – wollastonite.

various clay minerals (Tab. 5). In such rocks, olivine is usually replaced with a greenish clay mineral of a smectite chemistry, and the interstitial glass is altered into a yellowish-brown clay mineral of Fe-saponite chemistry or bright-green clay mineral of Fe-rich celadonite composition. A detailed identification of these clay minerals would require a separate XRD study.

CARBONATES

Carbonates represent a widespread secondary constituent of the volcanic rocks. These minerals are characteristic components of pseudomorphs after ferromagnesian minerals and plagioclase, but are also widespread in the groundmass. The analysed carbonates show a variable

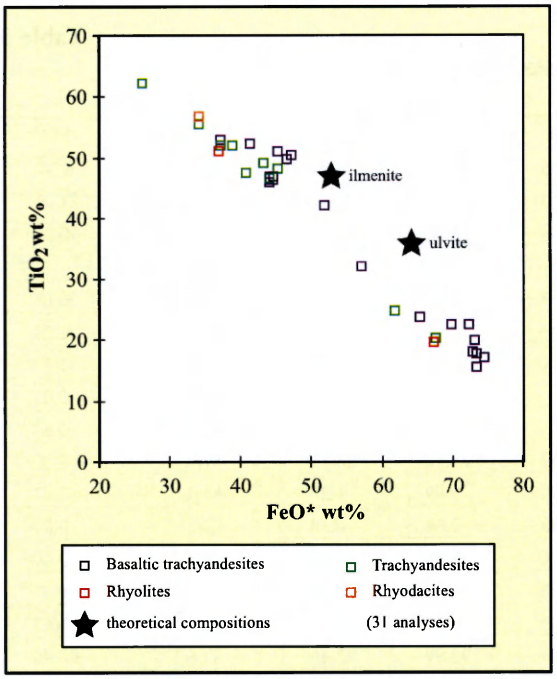

Fig. 14. Variation of Fe-Ti oxide composition in the volcanic rocks (most analyses with a low total: 90–95%).

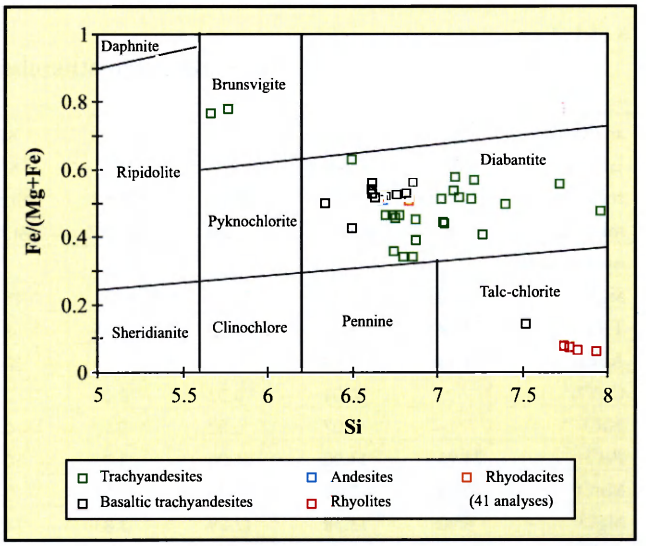

Fig. 15. Variation of chlorite composition in the volcanic rocks in the Hey diagram (1954).

composition (Tab. 6). Calcite and dolomite are the most common, and they usually contain significant Fe and Mn admixtures (up to 1 cation per formula unit each). Ca-rich dolomite is characteristic of pseudomorphs after pyroxenes in the andesites. Syderite and ankerite have been analysed in the trachyandesite and basaltic trachyandesite samples, both as pseudomorphs and interstitial components.

GEOCHEMISTRY

ANALYTICAL METHODS

The major and trace element chemistry of the volcanic rocks was determined by the X-ray fluorescence technique (XRF). Altogether, 105 samples were analysed, mostly using the Philips PW2400 and PW1480/10 spectrometers at the BGS, Keyworth, UK (91 samples) and partly on the ARL8420 spectrometer at the Geology Departament of Keele University, UK (14 samples). Representative analyses of the volcanic rocks of all the lithological units distinguished are given in Table 7.

POST-MAGMATIC ALTERATION AND ELEMENT MOBILITY

An important problem met during geochemical studies of ancient volcanic rocks is the alteration of their original chemical composition related to various post-magmatic processes (e.g. devitrification, hydrothermal activity, weathering). Numerous studies of volcanic and metavolcanic rocks world-wide (e.g. Winchester & Floyd, 1977, Howells *et al.*, 1991 and references therein) have documented that major elements such as silica and alkalis (Na, K), trace elements of the Large Ion Lithophile (LIL) group (e.g. Ba, Rb, Sr) and the transitional metals (Cr, V, Ni) are most prone to mobility on alteration, while trace elements of the High Field Strength (HFS) group (e.g. Th, Zr, Hf, Ti, Y, Nb) and most of the Rare Earth Elements (REE) remain 'immobile' even at high degrees of alteration or metamorphism.

The petrographic characteristics of the volcanic rocks of the Intra-Sudetic Basin show that many of them were subjected to a strong post-magmatic alteration. Although alteration and element mobility were not the subjects of this study, the observed geochemical variation seems to follow the well established general rules outlined above. However, a comparison of element concentrations in fresh and altered rocks (e.g. Awdankiewicz, 1997a) shows that the abundance of the 'mobile' elements in the moderately altered samples can still be considered as close to, and representative for, the original magmatic values. The most altered samples, with strongly modified chemical composition, can easily be identified within the data set by their unusual compositional patterns (e.g. four samples of silica-depleted basaltic andesites in Figure 16 a, basaltic trachyandesite sample US1 in Figure 19 and andesite samples in Figure 20, strongly depleted in Sr, K and Rb). In summary it is considered that although the post-magmatic alteration resulted in mobility of some elements, the original magmatic trends are generally well preserved and recognisable, especially if the most strongly altered samples are excluded.

CLASSIFICATION OF THE VOLCANIC ROCKS

The volcanic rocks have been classified according to the total alkali - silica (TAS) diagram (Le Maitre *et al.*, 1989). Because of the hydrothermal alteration present, this classification was checked against the Zr/TiO_2-Nb/Y

Table 3

Representative chemical analyses of micas

analysis	326	611	612	628	629	554	73	274
sample	5.43	Ch1	Ch1	SL6	SL6	3.155	5.59	5.7
rock unit	SGRd	ChRd	ChRd	SLRd	SLRd	BuTa	RGR	TR
mineral	Bt, P	Bt, PC	Bt, PR	Bt, PC	Bt, PR	Bt, G	Bt, P	Bt, G
oxides, wt%								
SiO_2	36.20	36.41	36.43	45.91	45.42	40.98	35.48	35.03
TiO_2	3.44	4.67	5.72	6.35	8.42	3.14	2.64	0.00
Al_2O_3	14.45	14.95	14.70	21.14	20.79	10.50	17.54	19.66
Cr_2O_3		0.01	0.02	0.00	0.00			
NiO		0.07	0.02	0.10	0.00			
FeO	23.95	14.90	16.00	9.27	10.43	12.67	25.18	26.71
MnO	0.78	0.10	0.26	1.38	0.04	0.00	1.69	1.27
MgO	6.90	13.38	12.09	3.83	4.13	16.82	0.66	0.78
CaO	0.00	0.00	0.00	0.27	0.30	0.00	0.00	0.00
Na_2O	0.60	0.71	0.71	1.26	0.14	0.78	0.86	0.46
K_2O	8.94	9.31	9.09	7.81	7.74	9.45	8.94	8.55
Total	95.26	94.51	95.04	97.32	97.41	94.34	92.99	92.46
cations per formula unit								
Si^{IV}	5.673	5.507	5.505	6.315	6.223	6.104	5.742	5.696
Al^{IV}	2.327	2.493	2.495	1.685	1.777	1.843	2.258	2.304
Ti^{IV}	0.000	0.000	0.000	0.000	0.000	0.053	0.000	0.000
T site	8.000	8.000	8.000	8.000	8.000	8.000	8.000	8.000
Al^{VI}	0.342	0.172	0.123	1.742	1.580	0.000	1.087	1.464
Ti^{VI}	0.405	0.531	0.650	0.657	0.868	0.290	0.321	0.000
Fe^{+2}	3.139	1.885	2.022	1.066	1.195	1.578	3.408	3.632
Cr		0.001	0.002	0.000	0.000			
Mn	0.104	0.013	0.033	0.161	0.005	0.000	0.232	0.175
Ni		0.009	0.002	0.011	0.000			
Mg	1.612	3.017	2.723	0.785	0.844	3.735	0.159	0.189
O site	5.602	5.619	5.553	4.411	4.492	5.603	5.207	5.460
Ba						0.037		
Ca	0.000	0.000	0.000	0.040	0.044	0.000	0.000	0.000
Na	0.182	0.208	0.208	0.336	0.037	0.225	0.27	0.145
K	1.787	1.796	1.752	1.37	1.353	1.796	1.846	1.774
A site	1.969	2.004	1.96	1.746	1.434	2.058	2.116	1.919

analysis	311
sample	5.36
rock unit	RGR
mineral	Ms, P
oxides, wt%	
SiO_2	50.66
TiO_2	0.20
Al_2O_3	31.59
Fe_2O_3	0.00
FeO	0.62
MnO	0.00
MgO	0.93
CaO	0.00
Na_2O	0.00
K_2O	9.35
H_2O	4.61
Total	97.96
cations p.f.u.	
Si^{IV}	6.741
Al^{IV}	1.259
T site	8.000
Al^{VI}	3.695
Ti	0.020
Fe^{+2}	0.069
Mn	0.000
Mg	0.184
O site	3.968
Ca	0.000
Na	0.000
K	1.587
A site	1.587

Numbers of cations based on 23 O with total Fe = Fe^{+2}.
Rock units: SGRd – Sady Górne rhyodacites, ChRd – Chełmiec rhyodacites, SLRD – Stary Lesieniec rhyodacites, BuTa – Bukowiec trachyandesites, GłTa – Gluszyca trachyandesites, RGR – Rusinowa-Grzmiąca rhyolites, TR – Trójgarb rhyolites.
Minerals: Bt – biotite, Ms – white mica, P – phenocryst (C – core, R – rim), G – groundmass grain.

plot, based on immobile trace elements (Winchester & Floyd, 1977). These classifications are shown in Figure 16.

The older volcanic suite of the Intra-Sudetic Basin consists of basaltic andesites, andesites and rhyodacites. These rocks are clearly distinguished on the Zr/TiO_2-Nb/Y diagram. On the TAS diagram the intermediate-composition samples are scattered from the andesite through to foidite fields. This scatter apparently results from silica depletion on alteration: all these samples are characterised by high LOI values (5–15%), reflecting the replacement of the primary magmatic silicates by volatile-rich minerals (carbonates, chlorites and clay minerals). However, samples with the lowest LOI (and the original igneous minerals, e.g. plagioclase, partly preserved), plot correctly in the basaltic andesite and andesite fields. The acidic samples, found in the rhyodacite/dacite and rhyolite fields on the Zr/TiO_2-Nb/Y diagram, plot in the rhyolite field on the TAS diagram. These samples possibly suffered some silica enrichment on alteration.

The younger volcanic suite consists of three major, chemically distinctive rock groups of basic, intermediate and acidic composition. These groups are clearly visible on both the Zr/TiO_2-Nb/Y and TAS diagrams and, according to the latter, the rocks are classified as basaltic trachyandesites, trachyandesites and rhyolites. Most of these samples show only weak to moderate alteration in

Table 4

Representative chemical analyses of opaque minerals

analysis	501	615	781	646	647	680	351	616	784	799	410
sample	5.50	Ch1	3.83	3.55	3.55	L4	4.52	Ch1	3.83	3.84	3.141
rock unit	NA	CHRd	KGBTa	GTa	GTa	ŁgR	GSRT	ChRd	KGBTa	LSBTa	GlTa
mineral	CrSp, ip	Mt, P	Mt, ip	Mt, G	Mt, G	Mt, G	Mt, P	Ilm, iP	Ilm, ip	Ilm, G	Ilm, P
oxides, wt%											
SiO2	0.00	0.41	0.11	2.88	0.27	0.22	0.38	0.20	0.11	0.01	0.61
TiO2	1.14	5.77	22.75	24.79	11.36	2.21	19.82	56.90	49.78	50.41	48.20
Al2O3	23.65	0.75	1.86	1.06	0.48	1.55	0.31	0.17	0.11	0.03	0.20
Cr2O3	37.02	0.05	0.00	0.06	0.04	0.00	0.00	0.06	0.00	0.00	0.00
NiO	0.00	0.14	0.00	0.01	0.03	0.06	0.00	0.00	0.00	0.00	0.00
Fe2O3	6.07	52.26	24.67	8.44	42.08	58.84	26.56	0.00	9.04	5.47	5.50
FeO	16.96	34.09	47.54	54.25	38.73	31.86	43.45	33.99	38.34	42.08	40.22
MnO	0.00	0.40	0.76	0.54	0.43	0.12	1.71	0.33	0.76	0.75	2.65
MgO	11.96	0.15	2.13	0.33	0.09	0.11	0.45	0.09	3.17	1.35	0.49
CaO	0.49	0.15	0.10	0.32	0.43	0.02	0.00	0.05	0.05	0.11	0.14
Na2O	0.00	0.04	0.22	0.00	0.00	0.00	0.49	0.00	0.01	0.00	0.00
K2O	0.00	0.01	0.01	0.04	0.12	0.00	0.00	0.01	0.03	0.00	0.00
Total	97.29	94.08	100.15	92.71	94.03	94.93	93.17	91.80	101.40	100.21	98.01
cations per formula unit											
Si	0.000	0.017	0.004	0.114	0.011	0.009	0.015	0.005	0.003	0.000	0.016
Al	0.879	0.035	0.081	0.049	0.023	0.073	0.014	0.005	0.003	0.001	0.006
Ti	0.027	0.175	0.625	0.737	0.344	0.066	0.596	1.114	0.913	0.947	0.929
Fe+3	0.144	1.585	0.678	0.251	1.274	1.773	0.799	0.000	0.166	0.103	0.106
Fe+2	0.447	1.149	1.452	1.793	1.303	1.067	1.453	0.740	0.782	0.880	0.862
Cr	0.923	0.002	0.000	0.002	0.002	0.000	0.000	0.001	0.000	0.000	0.000
Mn	0.000	0.014	0.024	0.018	0.014	0.004	0.058	0.007	0.016	0.016	0.058
Ni	0.000	0.006	0.000	0.000	0.001	0.002	0.000	0.000	0.000	0.000	0.000
Mg	0.563	0.009	0.116	0.019	0.005	0.006	0.027	0.003	0.116	0.05	0.019
Ca	0.017	0.006	0.004	0.014	0.018	0.001	0.000	0.001	0.001	0.003	0.004
Na	0.000	0.003	0.016	0.000	0.000	0.000	0.038	0.000	0.000	0.000	0.000
K	0.000	0.001	0.001	0.002	0.006	0.000	0.000	0.000	0.001	0.000	0.000
Total	3.000	2.996	3.001	2.999	3.000	2.999	3.000	1.876	2.001	2.000	2.000

Spinel analyses normalized to 3 cations. Ilmenite analyses (784, 799, 410) normalized to 2 cations, in analysis 616 number of cations on the basis of 3 O with total Fe = Fe^{+2}.
Rock units: NA – Nagórnik andesites, ChRd – Chelmiec rhyodacites, KGBTa – Kamienna Góra basaltic trachyandesites, LUBTa – Lesieniec-Unisalaw basaltic trachyandesites, GTa – Grzędy trachyandesites, GłTa – Gluszyca trachyandesites, ŁgR – Ługowina rhyolites, GSRT – Góry Suche rhyolitic tuffs.
Minerals: CrSp – chromian spinel, Mt – magnetite and titanomagnetite, Ilm – ilmenite, P – phenocryst, G – groundmass crystal, ip – inclusion in phenocryst.

thin sections and, consistently, the LOI values are rather low (usually <2.5%, rarely up to 5%).

The rhyolites of the younger suite show a significant geochemical variation and are further subdivided into low- and high-silica types, with 66–74% SiO_2 and 72–83% SiO_2, respectively (Fig. 17). This subdivision fits the geological relationships well: the low silica rhyolites form lavas and domes in the western and central parts of the Intra-Sudetic Basin, while the high-silica rhyolites are represented by tuffs and small subvolcanic intrusions in the central and eastern parts of the basin (Fig. 2). Although some of the high-silica rhyolites (the Rusinowa–Grzmiąca rhyolites) plot in the comendite/pantallerite field on the Zr/TiO_2-Nb/Y plot, they show low HFSE content (e.g. Zr and Nb) compared with typical peralkaline rhyolites (Leat *et al.*, 1986) and they are better classified as transitional, alkaline/subalkaline rhyolites.

GEOCHEMICAL AFFINITIES OF THE VOLCANIC SUITES

The older and younger volcanic suites of the Intra-Sudetic Basin differ in their geochemical affinities. On the TAS diagram (Fig. 16) both suites straddle the boundary of the alkaline and subalkaline rock series, but samples of the younger suite plot at higher alkalis at a given silica level and, except for some high-silica rhyolites, above the

Table 5

Representative chemical analyses of chlorites and clay minerals

analysis	495	290	658	659	130	216	642	562		463	520	783
sample	5.50	5.12	US1	US1	3.142	3.222	3.55	5.69		3.168	3.104	3.83
rock unit	NA	SLRd	LSBTa	LSBTa	GłTa	SWTa	GTa	GKR		LSBTa	KGBTa	KGBTa
mineral	Dia, ps	Dia, ps	Dia, ps	Dia, v	Dia, ps	Dia, ps	Bru, ps	TC, ps		Cel, I	?Sap, I	?Sm, ps
oxides, wt%												
SiO_2	32.02	32.73	31.91	30.59	31.85	31.40	26.10	43.29	SiO_2	55.40	48.11	47.90
TiO_2	0.00	0.00	0.09	0.04	0.00	0.00	0.05	0.00	TiO_2	0.00	0.00	0.12
Al_2O_3	17.73	17.98	15.55	11.85	10.63	11.54	22.11	28.12	Al_2O_3	5.96	5.33	1.55
Cr_2O_3			0.02	0.21			0.04		Cr_2O_3			
FeO	23.06	21.89	23.29	31.38	26.82	29.88	34.23	1.84	FeO	14.91	16.40	32.20
MnO	0.00	0.00	0.17	0.14	0.00	0.00	0.08	0.00	MnO	0.00	0.00	0.16
NiO			0.00	0.06			0.13		NiO			
MgO	12.36	11.84	17.42	13.77	14.10	12.95	5.69	11.81	MgO	6.70	16.70	7.22
CaO	0.47	0.59	0.39	0.06	0.59	0.48	0.32	0.70	CaO	0.00	1.51	0.65
Na_2O	0.38	0.29	0.01	0.02	0.35	0.31	0.00	0.00	Na_2O	0.00	0.30	0.00
K_2O	0.38	0.00	0.16	0.01	0.00	0.00	0.03	0.53	K_2O	9.42	0.77	0.04
Total	86.40	85.32	89.01	88.13	84.34	86.56	88.78	86.29	Total	92.39	89.12	89.84
cations per formula unit												
Si^{IV}	6.680	6.833	6.494	6.616	7.027	6.852	5.663	7.744	Si^{IV}	8.140	7.220	7.680
Al^{IV}	1.320	1.167	1.506	1.384	0.973	1.148	2.337	0.256	Al^{IV}	0.000	0.780	0.290
T site	8.000	8.000	8.000	8.000	8.000	8.000	8.000	8.000	Ti^{IV}	0.000	0.000	0.010
Al^{VI}	3.040	3.257	2.224	1.636	1.791	1.820	3.317	5.673	T site	8.140	8.000	7.980
Ti	0.000	0.000	0.014	0.007	0.000	0.000	0.008	0.000	Al^{VI}	1.030	0.160	0.000
Fe^{+2}	4.023	3.822	3.964	5.676	4.948	5.453	6.211	0.275	Ti^{VI}	0.000	0.000	0.000
Cr			0.003	0.036			0.007		Fe^{+2}	1.830	2.060	4.320
Mn	0.000	0.000	0.029	0.026	0.000	0.000	0.015	0.000	Mn	0.000	0.000	0.020
Ni			0.000	0.010			0.023		Mg	1.470	3.730	1.730
Mg	3.844	3.685	5.285	4.440	4.637	4.213	1.840	3.149	O site	4.330	5.950	6.060
Ca	0.105	0.132	0.085	0.014	0.139	0.112	0.074	0.134	Ca	0.000	0.240	0.110
Na	0.154	0.117	0.004	0.008	0.150	0.131	0.000	0.000	Na	0.000	0.090	0.000
K	0.101	0.000	0.042	0.003	0.000	0.000	0.008	0.121	K	1.760	0.150	0.010
O site	11.267	11.013	11.650	11.846	11.665	11.729	11.480	9.352	A site	1.760	0.480	0.120

For chlorites (analyses 495 to 562) numbers of cations based on 28), and for clay minerals (analyses 463 to 783) on 8 O, with total Fe = FeO in both cases.
Rock units: NA – Nagórnik andesites, SLRd – Stary Lesieniec rhyodacites, KGBTa – Kamienna Góra basaltic trachyandesites, LSBTa – Lesieniec-Unislaw basaltic trachyandesites,, GTa – Grzędy trachyandesites, GłTa – Gluszyca trachyandesites, SWTa – Stożek Wielki trachyandesites, GKR – Góry Krucze rhyolites.

subalkaline/alkaline divide of Kuno (1966). In contrast, samples of the older suite plot below this line (with the exception of 4 basaltic andesite samples, strongly depleted in silica due to alteration). Consistently with the major element data, the rocks of the older suite are characterised by lower Nb/Y ratios (largely <0.67), and those of the younger suite by higher Nb/Y ratios (largely >0.67), typical of the subalkaline and alkaline series, respectively (Fig. 16 b). On the AFM diagram (not show here), used for the further subdivision of the subalkaline series, the older suite plots largely in the calc-alkaline field. The geochemical characteristics discussed above point to a subalkaline, most probably calc-alkaline affinity of the older suite, and a mildly alkaline affinity of the younger suite.

The contrasting geochemical characteristics of the two suites are further illustrated in Figure 18. Compared with the calc-alkaline suite, the alkaline suite shows, in general, higher contents of Zr, Nb, Y and Ti, with lower V, Cr and Ni content (Tab. 7). The geochemical characteristics of the older suite compare well with those typical of volcanic arc lavas, while the younger suite largely shows features typical of within-plate lavas, but with mixed arc/within-plate characteristics in some of the high silica rhyolites.

The MORB-normalised patterns of the basaltic andesites and basaltic trachyandesites, which are the most primitive rock types of the calc-alkaline and mildly alkaline suite, respectively, have been compared in Figure 19. The shapes of the basaltic andesite and basaltic trachyandesite patterns are very similar and the main differences are in trace element contents and the slope of the patterns. The basaltic andesites are characterised by lower conetnts

Table 6

Representative chemical analyses of carbonates

analysis	492	493	496	617	444	661	201	213	366	381
sample	5.50	5.50	5.50	Ch1	3.168	US1	3.179	3.222	G7.4	G7.4
rock unit	NA	NA	NA	ChRd	LSBTa	LSBTa	RGTa	SWTa	GTa	GTa
mineral	Cal, ps	Dol, ps	Dol, ps	Cal, ps	Ank, I	Cal, ps	Ank, ps	Cal, ps	Syd, ps	Cal, ps
oxides, wt%										
SiO_2	0.57	0.74	0.54	0.08	0.95	0.00	0.39	1.33	2.26	0.00
TiO_2	0.00	0.00	0.00	0.01	0.00	0.00	0.00	0.00	1.01	0.00
Al_2O_3	0.00	0.00	0.00	0.06	0.00	0.03	0.00	0.24	0.49	0.00
FeO	1.74	3.22	3.82	0.34	8.37	0.02	14.38	6.32	47.55	0.00
MnO	4.37	6.18	3.54	0.95	0.98	0.69	4.25	1.18	0.00	0.00
MgO	1.54	8.17	13.43	0.22	14.17	0.02	8.54	1.49	0.00	0.74
CaO	47.15	33.94	29.96	55.33	26.17	56.79	24.63	41.50	1.07	51.97
Na_2O	0.00	0.00	0.00	0.00	0.00	0.00	0.26	0.00	0.29	0.00
K_2O	0.00	0.00	0.00	0.03	0.00	0.00	0.00	0.11	0.00	0.00
total	55.37	52.25	51.29	57.02	50.64	57.55	52.45	52.17	52.67	52.71
cations per formula unit										
Si	0.058	0.077	0.055	0.008	0.097	0.000	0.042	0.142	0.282	0.000
Al	0.000	0.000	0.000	0.007	0.000	0.003	0.000	0.030	0.072	0.000
Ti	0.00	0.000	0.000	0.001	0.000	0.000	0.000	0.000	0.095	0.000
Fe^{+2}	0.148	0.279	0.323	0.028	0.713	0.002	1.294	0.565	4.961	0.000
Mn	0.376	0.542	0.303	0.079	0.085	0.057	0.387	0.107	0.000	0.000
Mg	0.233	1.261	2.023	0.032	2.152	0.003	1.369	0.237	0.000	0.117
Ca	5.128	3.765	3.243	5.831	2.857	5.928	2.839	4.753	0.143	5.883
Na	0.000	0.000	0.000	0.000	0.000	0.000	0.054	0.000	0.070	0.000
K	0.000	0.000	0.000	0.004	0.000	0.000	0.00	0.015	0.000	0.000
Total	5.943	5.924	5.947	5.990	5.904	5.997	5.985	5.849	5.623	6.000

Numbers of cations on the basis of 6 O. Total Fe = Fe^{+2}.
Rock units: NA – Nagórnik andesites, ChRd – Chełmiec rhyodacites, LSBTa – Lesieniec-Unisław basaltic trachyandesites, RGTa – Rusinowa-Grzmiąca trachyandesites, SWTa – Stożek Wielki trachyandesites, GTa – Grzędy trachyandesites.
Minerals: Ank – ankerite, Cal – calcite, Dol – dolomite, Syd – syderite, ps – pseudomorph, I – interstitial aggregate.

of all elements but Cr, the Nb to Y segment of the patterns is gently inclined with a distinctive spike at Ce, and K, Rb and Ba are strongly enriched relative to the other elements. These features make the patterns similar to those of calc-alkaline basalts erupted at active continental margins (Pearce, 1983). The basaltic trachyandesites are characterised by higher trace element contents and a stronger enrichment of LILE, Th, Nb and LREE relative to Zr and Y. These patterns compare better to within plate lavas, except for the small Nb depletion relative to Th and Ce, more typical of destructive plate margin lavas or intraplate lavas contaminated with continental crust components (Pearce, 1983).

The data discussed above demonstrate that the geochemical features of the volcanic rocks emplaced within the Intra-Sudetic Basin during the late Palaeozoic changed with time. The older volcanic suite, emplaced in the early and late Carboniferous, shows calc-alkaline, destructive plate margin-like affinities, and it is strongly dominated by silicic rocks. The younger suite, erupted in the late Carboniferous and early Permian, shows mildly alkaline, within-plate characteristics, with some gradations towards destructive plate margin-like features. Compared with the older suite, the younger one contains more abundant basic and intermediate rocks.

GEOCHEMICAL VARIATION WITHIN THE SUITES

The MORB-normalised trace element patterns of the volcanic rocks of the calc-alkaline and mildly alkaline suites are shown in Figures 20 and 21, respectively. Within each of the suites, the trace element patterns of the more evolved rocks are similar to those of the less evolved rocks in terms of their general shape and slope. The patterns of the basic and intermediate rocks are relatively smooth, but, with increasing silica content, negative anomalies in Sr, P, Nb and Ti become more pronounced. Many of the acidic rocks also show Ba, Zr and Hf depletion, and the most evolved rhyolites also show light REE (e.g. Ce) depletion or Th depletion. Well defined variation trends with increasing silica content are also seen in Harker diagrams (i.e. element vs. SiO_2 diagrams). This variation is further discussed in the next chapters.

Table 7

Representative chemical analyses of the volcanic rocks

older volcanic suite									*younger volcanic suite*						
Sample	B79*	B101*	5.54	5.48	5.49	5.24	5.13	5.14	3.114	3.83	3.84	US1	3.155	3.173	3.142
Rock	BA	BA	A	Rd	Rd	Rd	Rd	Rd	BTa	BTa	BTa	BTa	Ta	Ta	Ta
Unit	BBA	BBA	NA	SGRd	SGRd	ChRd	SLRd	SLRd	KGBTa	KGBTa	LSBTa	LSBTa	BuTa	BuTa	GlTa
wt%															
SiO_2	34.13	49.96	51.92	74.86	69.23	72.95	69.84	71.18	50.18	51.48	51.09	53.47	57.14	57.71	57.55
TiO_2	1.36	1.07	0.83	0.10	0.57	0.19	0.44	0.28	2.48	2.45	2.46	2.35	1.52	1.47	1.40
$Al2O_3$	17.52	16.04	14.74	13.79	16.46	14.14	15.75	15.26	15.66	16.01	15.93	15.01	15.84	15.87	15.55
Fe_2O_3t	16.54	9.35	16.43	1.36	2.90	1.80	3.16	2.69	12.51	13.09	13.06	12.48	8.87	8.12	8.56
MnO	0.21	0.09	0.23	0.01	0.04	0.02	0.02	0.01	0.16	0.17	0.17	0.05	0.12	0.10	0.12
MgO	4.66	4.86	3.29	0.16	0.42	0.64	0.75	0.54	3.13	3.23	3.16	4.91	2.32	2.46	2.88
CaO	9.53	7.22	2.41	0.44	0.36	0.44	1.38	0.76	6.68	6.98	6.82	2.10	5.41	4.96	3.42
Na_2O	2.88	3.71	4.71	3.39	3.25	4.27	4.24	4.99	3.60	3.69	3.74	4.73	3.94	3.94	5.27
K_2O	0.46	0.66	0.19	4.92	3.77	3.59	3.23	3.00	1.93	1.93	1.94	0.24	2.96	2.96	3.21
P_2O_5	0.15	0.14	0.17	0.03	0.17	0.05	0.13	0.09	0.85	0.92	0.89	0.79	0.53	0.51	0.56
LOI	12.42	7.00	4.56	0.86	2.47	1.20	1.27	0.98	1.05	0.61	0.35	3.33	0.80	1.40	1.55
Total	99.86	100.10	99.48	99.92	99.64	99.29	100.21	99.78	98.23	100.56	99.61	99.46	99.45	99.50	100.07
ppm															
Ba	53	236	48	371	238	498	634	548	556	588	812	484	1338	1361	621
Ce	15	40	44	44	70	53	48	47	116	118	116	125	142	153	155
Co			17	2	8	3	3	2	30	30	29	33	19	19	22
Cr	1006	201	166	0	4	0	0	0	3	0	0	5	0	0	14
Cu	49	28	52	3	3	2	2	3	55	49	49	38	33	14	20
Hf			4	3	5	4	4	5	10	10	10	8	12	12	11
La	2	8	25	21	37	33	28	23	58	60	56	64	72	76	79
Nb	7	6	6	15	16	12	9	8	42	44	41	39	37	36	35
Nd	12	13	21	17	27	23	21	15	50	54	50	55	56	58	60
Ni	279	84	13	4	6	2	4	2	20	14	16	18	8	8	17
Pb	36	13	30	21	10	9	14	11	8	10	7	2	15	14	13
Rb	13	17	6	145	100	86	90	71	40	28	42	3	74	72	65
Sc			24	11	14	8	12	6	23	21	19	25	20	19	20
Sm			6	6	8	7	5	4	9	11	9	12	9	9	12
Sr	182	270	63	75	81	75	221	172	297	319	407	118	250	237	224
Ta			0	2	0	2	0	1	3	1	2	3	0	1	1
Th	2	0	5	10	9	9	7	6	6	7	6	7	11	11	11
U			3	3	2	3	2	1	0	0	1	2	2	4	2
V	269	179	174	7	48	14	27	10	147	144	151	176	101	97	109
Y	34	23	16	34	26	28	22	12	48	48	48	43	50	51	48
Zn	599	183	126	13	32	41	21	22	106	127	129	171	91	99	94
Zr	120	121	128	83	188	136	151	164	412	436	420	356	553	557	458

MAGMA ORIGIN AND DIFFERENTIATION

THE BASIC ROCKS

The basaltic andesites and the basaltic trachyandesites represent the most primitive members of the calc-alkaline and mildly alkaline suite, respectively. However, neither of these rocks can be considered primary mantle-derived magmas because of their relatively high silica contents, low magnesium numbers (#Mg = MgO/(MgO+FeO); ca. 0.35 in the basaltic andesites and ca. 0.26 in the basaltic trachyandesites), and low Cr and Ni content (Tab. 7), different from those expected for primary mantle melts (Wilson, 1989). Both of the discussed rock types thus represent relatively evolved magmas that originated from more primitive melts, most probably due to fractionation of olivine (responsible for Mg and Ni depletion) and spinel (resulting in Cr depletion). In addition, the relative Th and LILE enrichment and Nb depletion of the basaltic andesites and the basaltic trachyandesites point to a contribution of upper continental crust components in their genesis. This contribution might have resulted from: 1) assimi-

Table 7 (continued)

Representative chemical analyses of the volcanic rocks

younger volcanic suite															
Sample	3.55	3.180	3.219	3.235	5.69	3.241	L4	3.187	3.195	3.138	5.36	5.57	5.6	4.38	4.52
Rock	Ta	Ta	Ta	Ta	LSR	LSR	LSR	LSR	LSR	HSR	HSR	HSR	HSR	RT	RT
Unit	GTa	RGTa	SWTa	SWTa	GKR	DR	ŁgR	WR	WR	ŁR	RGR	RGR	TR	GSRT	GSRT
wt%															
SiO_2	58.11	62.70	60.51	57.10	71.92	74.70	71.12	68.57	66.45	74.68	78.29	76.93	76.26	78.08	75.66
TiO_2	1.25	0.91	0.98	1.38	0.12	0.09	0.23	0.50	0.37	0.14	0.04	0.12	0.01	0.08	0.13
Al_2O_3	14.94	14.55	14.93	16.44	13.88	12.25	13.94	13.98	15.30	12.84	11.96	12.51	13.57	11.08	12.51
Fe_2O_3t	4.80	6.34	6.38	7.86	2.08	1.68	3.13	4.64	4.57	1.71	0.72	1.42	0.46	0.57	1.44
MnO	0.15	0.10	0.12	0.03	0.01	0.01	0.02	0.03	0.02	0.00	0.00	0.00	0.01	0.01	0.02
MgO	0.73	1.73	1.83	3.74	1.05	0.48	0.41	0.42	0.48	0.25	0.12	0.34	0.06	1.39	0.54
CaO	7.72	1.92	3.69	1.02	0.22	0.22	0.62	1.05	0.40	0.37	0.03	0.09	0.08	0.06	0.09
Na_2O	3.81	3.82	3.43	2.51	1.34	1.88	3.27	3.45	2.60	3.17	1.48	1.72	0.31	0.27	0.79
K_2O	3.04	4.58	3.80	6.03	8.41	6.87	5.99	5.36	7.21	5.77	5.75	6.69	6.13	5.76	7.94
P_2O_5	0.50	0.35	0.38	0.52	0.03	0.03	0.06	0.17	0.09	0.03	0.01	0.02	0.02	0.01	0.02
LOI	4.87	1.60	3.54	3.08	1.25	0.94	0.65	0.86	1.21	0.51	1.32	0.96	2.34	2.09	1.09
Total	99.92	98.60	99.59	99.71	100.31	99.15	99.44	99.03	98.70	99.47	99.72	100.80	99.25	99.40	100.23
ppm															
Ba	1082	1426	1244	737	329	479	899	843	2094	116	101	112	56	59	98
Ce	136	172	166	182	146	89	339	171	269	113	4	137	18	26	159
Co	14	12	15	18	1	0	3	11	3	3	0	0	0	0	0
Cr	0	0	0	0	0	0	0	0	0	0	0	0	0	0	0
Cu	48	28	25	9	2	4	7	5	7	3	4	11	1	3	12
Hf	11	11	12	12	8	6	11	9	18	5	4	5	2	4	5
La	69	89	85	91	66	43	180	87	144	36	1	63	7	9	74
Nb	34	33	35	39	28	23	27	30	33	22	39	22	9	27	20
Nd	54	66	60	69	52	34	107	67	90	29	3	47	8	15	58
Ni	7	6	7	8	2	2	1	5	5	2	2	3	1	3	2
Pb	16	18	17	18	12	17	27	23	27	22	3	15	9	3	9
Rb	83	122	102	125	167	170	147	151	151	139	163	166	200	146	141
Sc	20	16	19	17	12	8	13	13	11	10	5	10	5	7	10
Sm	10	11	10	13	11	8	16	13	11	8	4	11	5	6	12
Sr	202	101	141	49	26	32	54	68	63	17	7	36	48	10	16
Ta	2	3	2	3	3	2	2	2	2	2	4	1	3	3	1
Th	12	16	12	11	22	17	25	18	19	19	17	19	4	15	20
U	2	3	5	3	5	3	2	3	5	3	3	4	3	1	3
V	83	56	65	84	3	9	5	27	10	4	8	9	2	10	4
Y	52	51	50	48	35	38	43	46	51	35	64	38	31	45	26
Zn	139	136	90	114	24	14	20	30	34	10	8	22	13	29	28
Zr	481	456	549	504	253	183	476	373	802	180	79	165	37	83	177

Samples B79 and B101 were analysed at Keele University, the rest at BGS, Keyworth, UK. Rocks: Ba – basaltic andesiye, A – andesite, Rd – rhyodacite, BTa – basaltic trachyandesite, Ta – trachyandesite, LSR – low-silica rhyolite, HSR – high-silica rhyolite, RT – rhyolitic tuff. Unit abbreviatios are explained in caption to Fig. 2.

lation of crustal rocks by the ascending primary magmas, or 2) metasomatic enrichment processes (e.g. subduction-related) that affected the mantle sources of the magmas. The geochemical effects can be very similar in both cases, but the distinction between the essentially different processes involved is problematic (Pearce, 1983; Wilson, 1989). This is considered to be the case for the rocks discussed here: the geochemical data presented in this paper do not allow an unequivocal conclusion on the problem to be drawn.

However, the geochemistry of the basaltic andesites and the basaltic trachyandesites provides some evidence on the origin of the parental magmas of these rocks. As discussed above, the trace element patterns show general similarities, but the basaltic trachyandesites are characterised by a higher content and a stronger enrichment of several incompatible trace elements (Fig. 19), consistent with their more alkaline major element chemistry (Fig. 16). These features suggest that the parental magmas of both rock types originated from similar mantle sources, but at

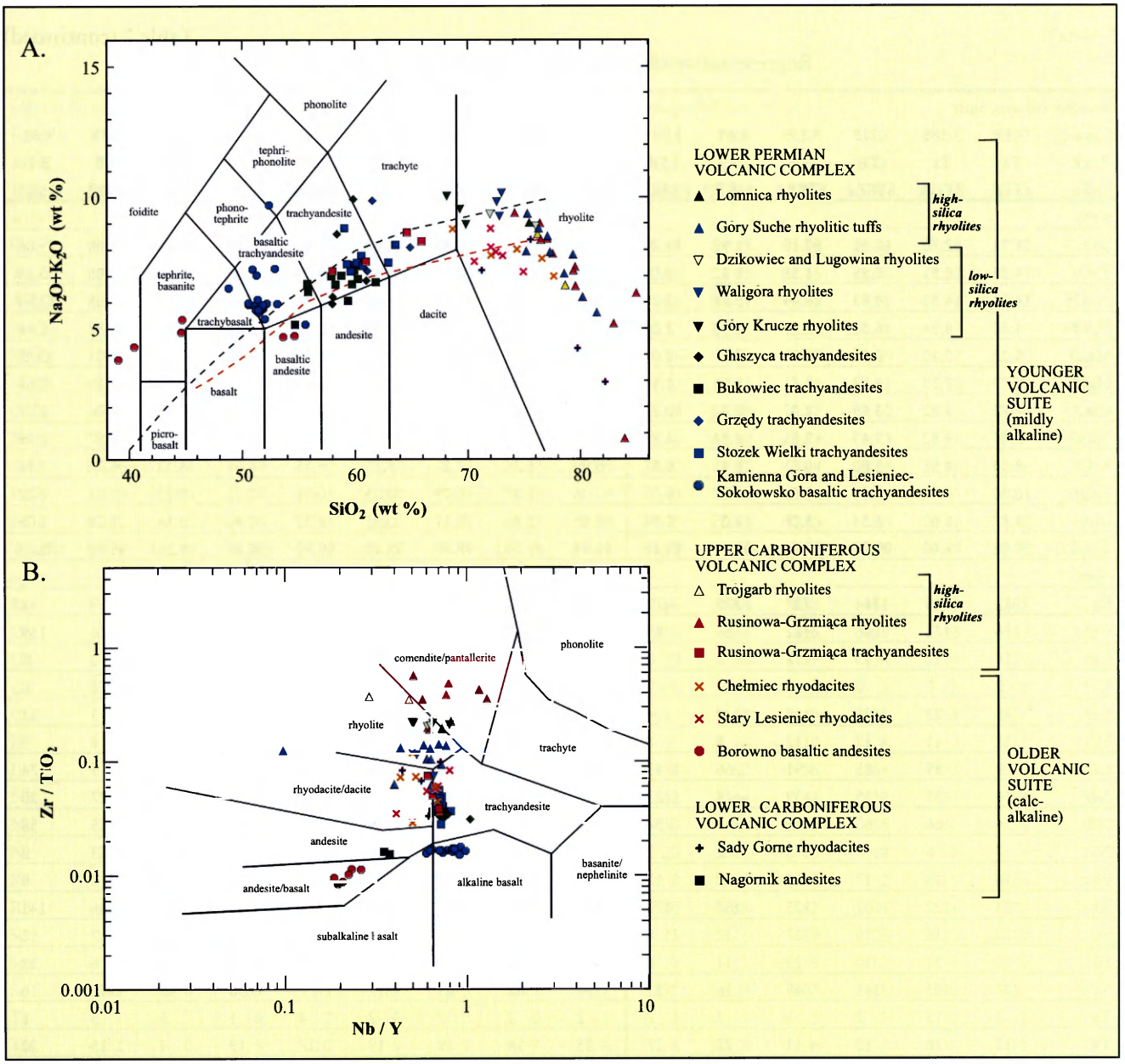

Fig. 16. Classification of the volcanic rocks of the Intra-Sudetic Basin. A – the total alkali-silica (TAS) diagram (after Le Maitre *et al.*, 1989). The broken lines show the boundary between the alkaline (above) and subalkaline (below) series (black line – Irvine and Baragar, 1971; red line – Kuno, 1966, vide Rollinson, 1993). B – the Zr/TiO_2 - Nb/Y diagram (after Winchester and Floyd, 1977).

different degrees of partial melting, lower for the basaltic trachyandesites. The relatively small LREE enrichment of both rock types (compared with strongly alkaline intraplate magmas) indicates that garnet was absent in the residues at the time the primary melts segregated from their mantle sources. This may suggest that either the melts originated at relatively low pressures and shallow depths (within the lithospheric mantle ?), from a spinel lherzolite source, or at higher pressures and depths, from a garnet lherzolite, but with garnet consumed by the magmas due to high degrees of partial melting. However, these possibilities cannot be easily verified, largely due to the evolved composition of the rocks, and even more complex models (e.g. generation of the melts at both different depths and degrees of melting) cannot be definitely excluded because too many factors remain speculative.

In summary it is considered that the basaltic andesites and the basaltic trachyandesites represent relatively evolved rocks that originated from different parental magmas. These parental, primary melts were derived from similar mantle sources at relatively shallow depths (possibly, from spinel lherzolites), at variable degrees of partial melting (lower for the parental melts of the basaltic trachyandesites) and fractionated olivine with spinel in the early stages of differentiation. Both the basaltic andesites and the basaltic trachyandesites contain a significant continental crustal component, either inherited from their mantle sources, or related to the assimilation of crustal rocks by their parental magmas.

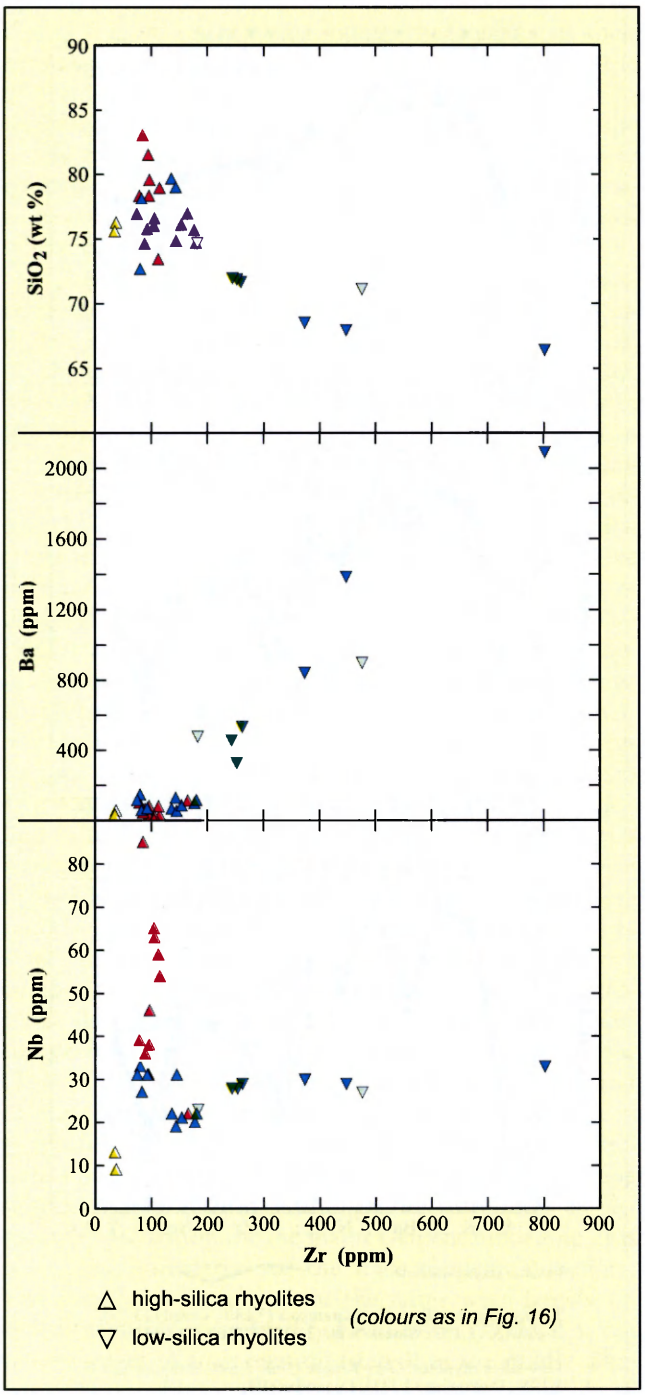

Fig. 17. Variation of selected elements in the rhyolites and their subdivision into high-silica and low-silica types. Symbols as in Figure 16.

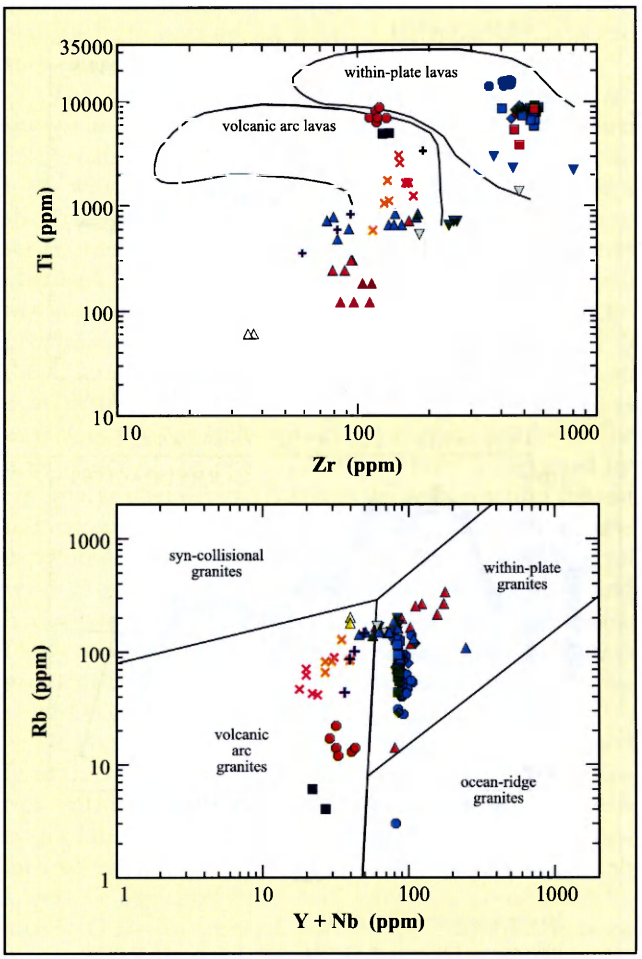

Fig. 18. Volcanic rocks of the Intra-Sudetic Basin on the Zr-Ti and Rb-(Y+Nb) discrimination diagrams (after Pearce, 1983, and Pearce *et al.*, 1984). Symbols as in Figure 16.

THE INTERMEDIATE AND ACIDIC ROCKS

The geochemical characteristics of the volcanic rocks discussed in the previous chapters point to strong similarities of the intermediate and acidic rocks to the associated more primitive rocks within each of the two suites. This strongly suggests close genetic links between the more evolved and more primitive compositions: the latter may be parental to the former. The nature of these genetic links is further constrained by the systematic geochemical

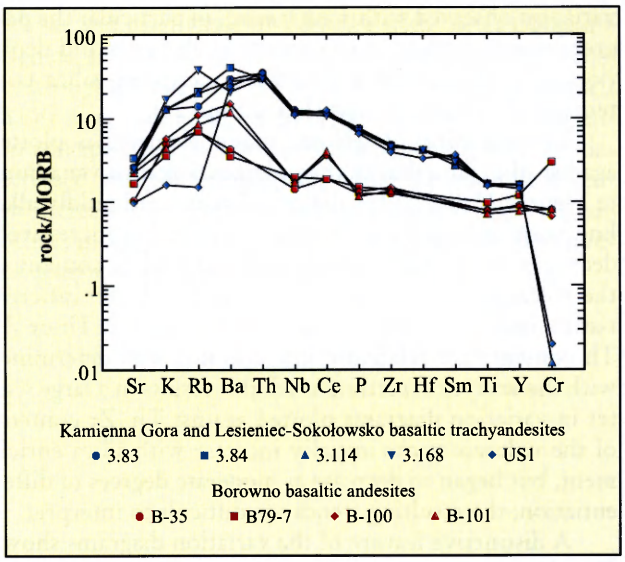

Fig. 19. MORB-normalised (after Pearce, 1983) trace element patterns of the basaltic andesites and basaltic trachyandesites.

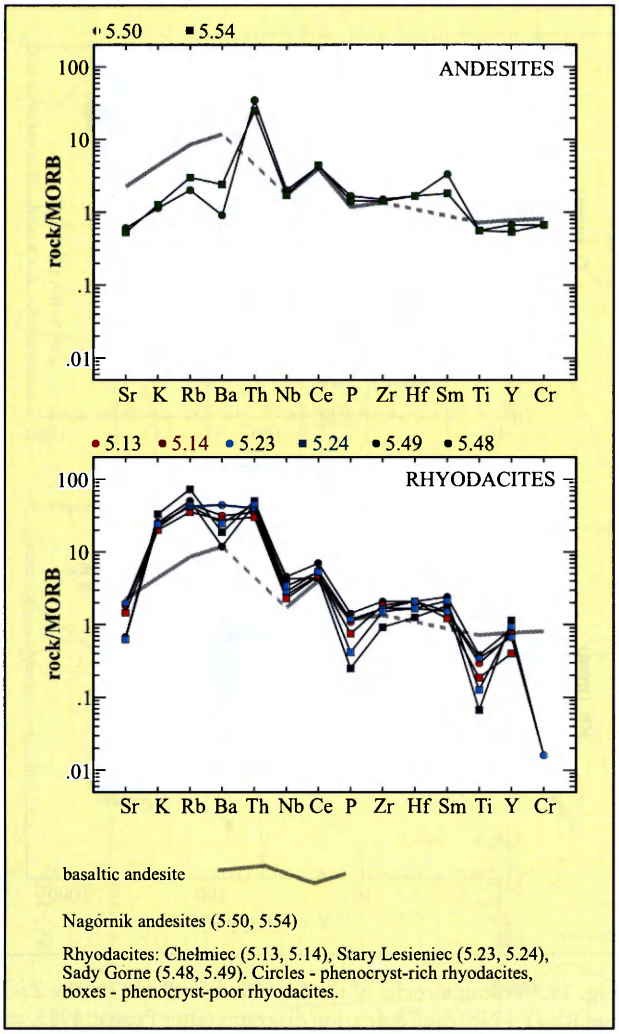

Fig. 20. MORB-normalised (after Pearce, 1983) trace element patterns of the andesites and rhyodacites. Basaltic andesite patterns shown for reference.

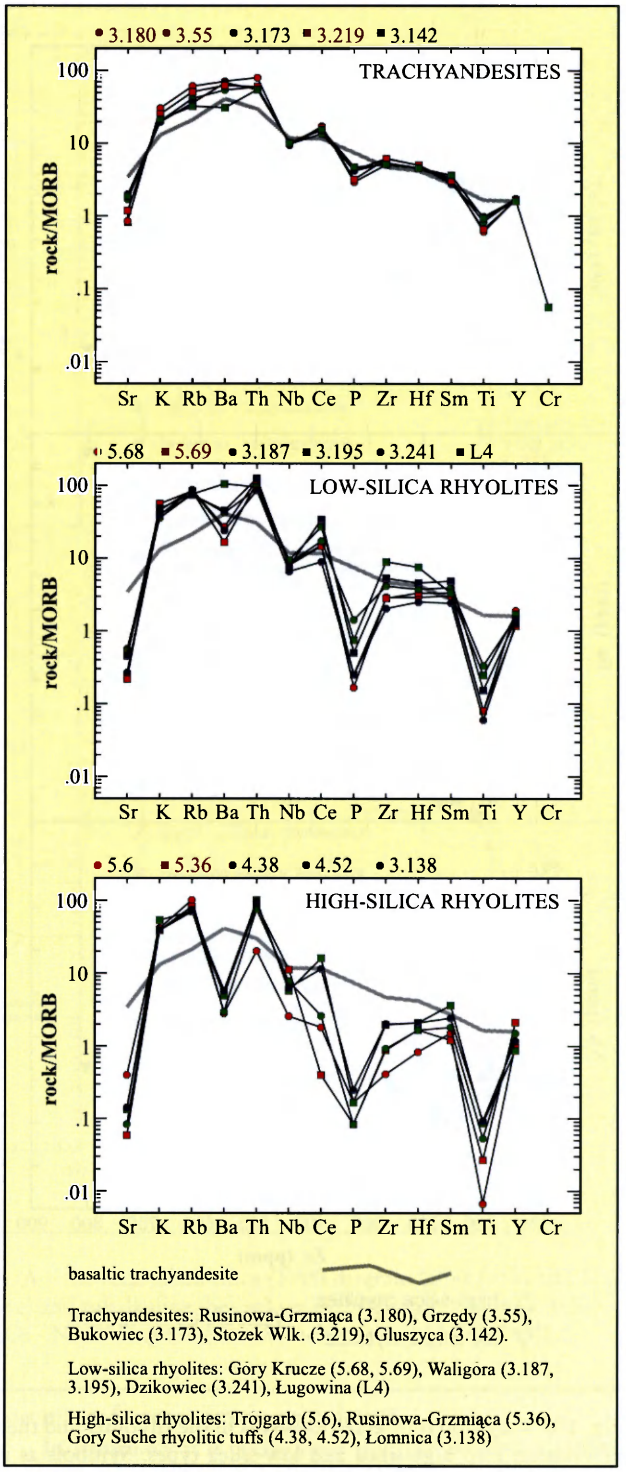

Fig. 21. MORB- normalised (after Pearce, 1983) trace element patterns of the trachyandesites and rhyolites. Basaltic trachyandesite patterns shown for reference.

variation observed within each suite, in particular the progressive enrichment in incompatible elements and depletion in compatible elements with increasing silica contents of the volcanic rocks (Fig. 20 and 21).

The variation of selected major elements is plotted against silica, and that of trace elements against vanadium, in Figures 22 and 23 for the calc-alkaline and mildly alkaline suite, respectively. Vanadium, which progressively decreases in abundance with increasing silica content of the volcanic rocks, has been found to be a better differentiation index that other trace elements, such as Th or Zr. Th contents are relatively low and not well determined with the analytical method used; this results in a large scatter in variation diagrams plotted against Th. Zr contents of the volcanic rocks initially increase with silica enrichment, but began to decrease at moderate degrees of differentiation; the resulting trends are difficult to interpret.

A distinctive feature of the variation diagrams shown (Fig. 22 and 23) is their segmented nature, with numerous inflection points: e.g. in the calc-alkaline suite at 70% and 60% SiO_2 for Al and P, respectively, and at 50 ppm of V for Zr and Ce; in the mildly alkaline suite at 60% and 73% SiO_2 for Al, at 75% SiO_2 for K, and at ca. 20 ppm of V for the trace elements. Such trends are interpreted (Cox *et al.*, 1979; Wilson, 1989) as the effect of crystal-liquid fractionation processes, apparently fractional crystallisation in this case. The inflection points mark the melt compositions at which the fractionating mineral assemblages

change, e.g. when successive minerals cease or start their crystallisation. The presence of the inflection points in the diagrams is consistent with changes in the phenocryst assemblages within the volcanic suites (Fig. 3). Thus, the geochemical and petrographic evidence are qualitatively consistent with the hypothesis that the geochemical variation within each of the suites is related to fractional crystallisation processes.

This hypothesis has been tested with simple numerical models. The major element variation was modelled using mass-balance calculations, and the Rayleigh fractionation equation was applied for the trace element modelling. These methods are described in Cox *et al.* (1979), Wilson (1989) and Rollinson (1993). Fractional crystallisation in each suite has been modelled in three steps: 1) from basaltic andesite (basaltic trachyandesite) to andesite (trachyandesite), 2) from andesite (trachyandesite) to primitive rhyodacite (low-silica rhyolite), and 3) from primitive rhyodacite (low-silica rhyolite) to evolved rhyodacite (high-silica rhyolite). For each step, initial melt compositions, fractionating mineral assemblages and their compositions, and partition coefficients for the trace elements, are given in Tab. 8. Initial melt compositions were generally the averages of the observed compositions of particular rock types (e.g. average basaltic trachyandesite for step 1, and average trachyandesite for step 2 in the mildly alkaline suite, etc.), and the most strongly altered samples were excluded (e.g. 4 samples of basaltic andesites with highest LOI). The fractionated mineral assemblages qualitatively corresponded to the phenocryst assemblages observed in the volcanic rocks, and the fractionated mineral compositions, when possible, were taken from the microprobe determinations (Tables 2, 3 and 4), or theoretical compositions equivalent to those measured were used (for Ol and Pl). In the calc-alkaline suite, where determination of the original composition of several minerals (e.g. pyroxenes and amphiboles) was not possible due to alteration, mineral compositions typical of the mildly alkaline suite were used instead. Although this introduces an element of speculation for the major element modelling, it is practically immaterial for the trace element modelling. The partition coefficients for the latter were largely selected from the compilation of Rollinson (1993). The advanced stages of fractionation (step 3) in the mildly alkaline suite possibly involved various accessory minerals, as monazite or xenotime, for which the partition coefficients of the trace elements are poorly constrained. However, allanite, with better known partition coefficients, was used to illustrate the possible influence of the accessory phases.

The calculated fractional crystallisation trends are shown in Figures 22 and 23. In both suites, the calculated fractionation paths fit the observed geochemical variation well, which is also true for several other elements not shown here. However, a good fit of the calculated and observed trends for all the elements in the data set was not obtained. The major reasons are possibly the following: 1) the numerical models applied represent only a crude approximation of the real differentiation processes, and 2) the differentiation processes might have taken place in an open system, with assimilation of crustal rocks, as well as mixing of various melts within the magma chambers. The importance of the open-system processes is suggested by e.g. quartz phenocrysts (xenocrysts) with reaction rims in the calc-alkaline volcanic rocks and disequlibrium textures observed in many phenocrysts in both suites (e.g. reverse compositional zoning in some feldspars, sieve and honeycomb textures in feldspars and other minerals). However, a reliable numerical modelling of these effects is problematic due to the numerous uncertain factors involved (e.g. the composition of contaminants).

In conclusion it is considered that the relatively good fit of the simple numerical models of fractional crystallisation with the observed geochemical variation suggests a rather limited role of the open system processes. The major and trace element variation of the volcanic rocks can largely be explained by closed-system fractional crystallisation. Different mineral assemblages fractionated from magmas in each of the suites, and the fractionating mineral assemblages and their composition (e.g. the An content of plagioclase) gradually changed with the progress of differentiation. The main fractionating minerals in the calc-alkaline suite were plagioclase and pyroxene and, at the advanced stages of fractionation, plagioclase with hornblende and biotite. In the mildly alkaline suite fractionating mineral assemblages changed from plagioclase and olivine, through plagioclase and pyroxenes, to K-feldspar and plagioclase. In contrast with the calc-alkaline magmas, anhydrous mineral assemblages were characteristic throughout the suite. In both suites the major mineral phases were accompanied by accessory Fe-Ti oxides, zircon and apatite. The amount of fractionating Fe-Ti oxides decreased with differentiation, while the amount of zircon increased. In addition, other accessory minerals (xenotime, monazite or others ?) fractionated from the rhyolitic magmas of the mildly alkaline suite.

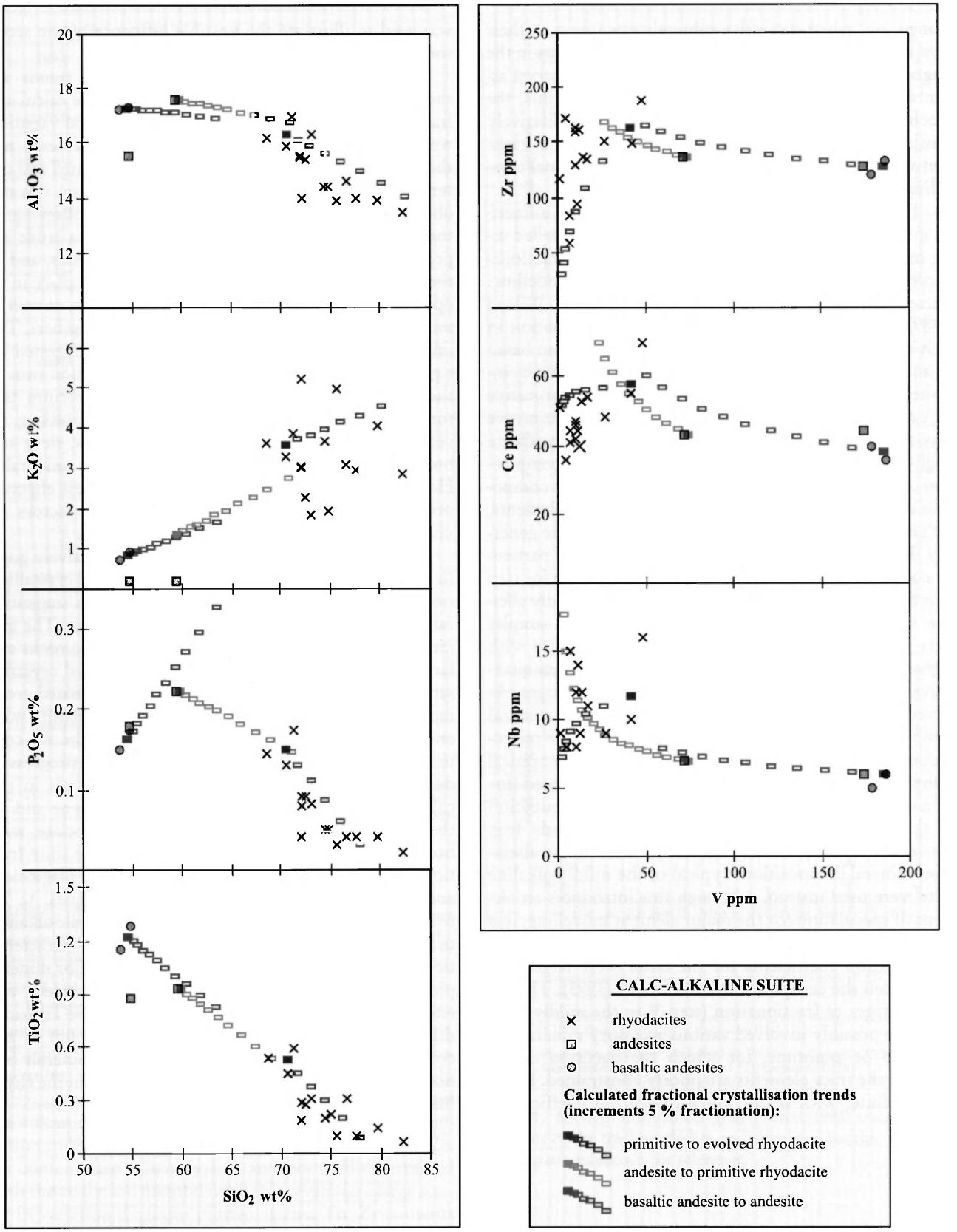

Fig. 22. Variation of selected major and trace elements in the calc-alkaline volcanic rocks and calculated fractional crystallisation paths (see text for details).

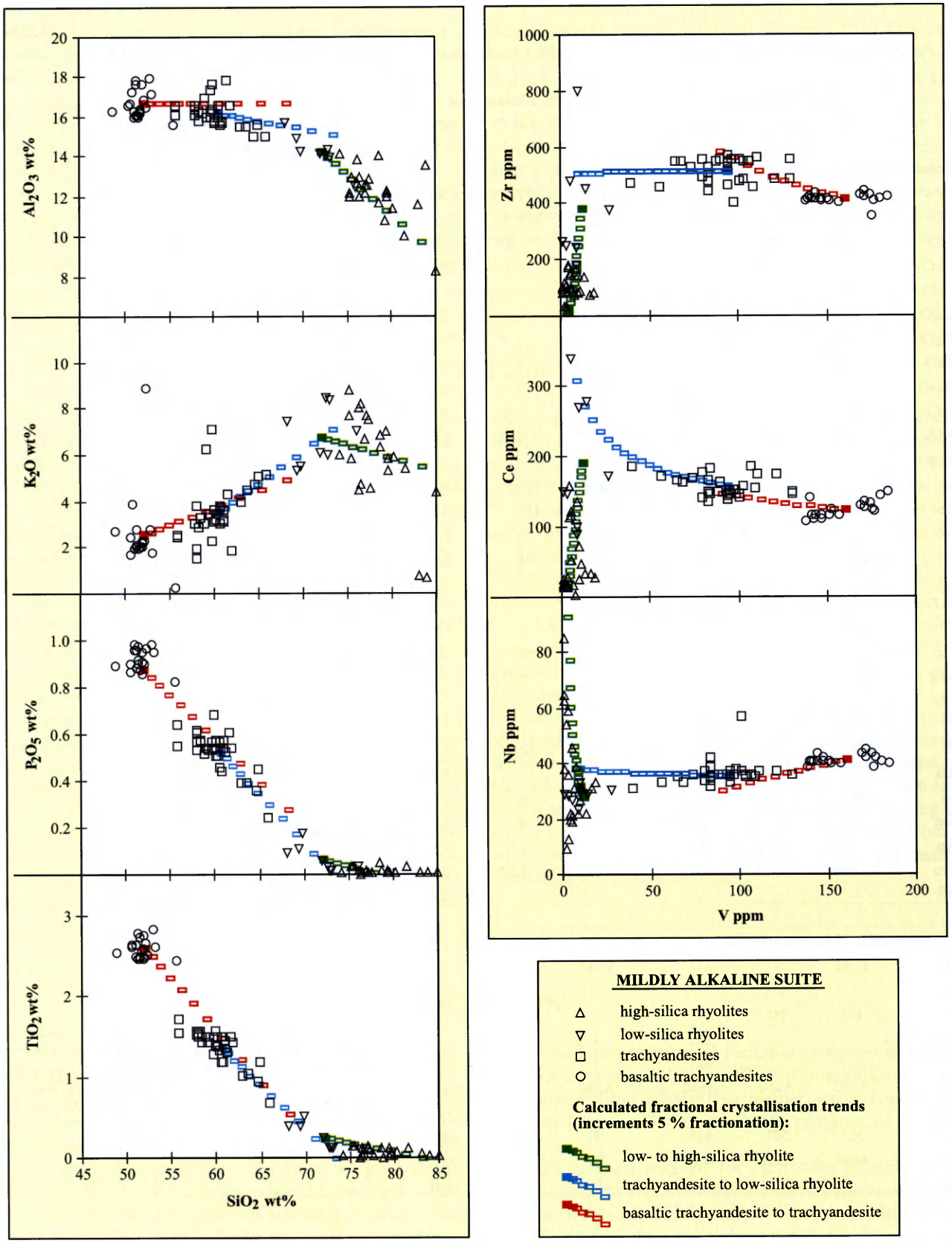

Fig. 23. Variation of selected major and trace elements in the mildly alkaline volcanic rocks and calculated fractional crystallisation paths (see text for details).

Table 8

Parameters used for the modelling of fractional crystallisation paths in the volcanic suites. Comments in the text

	Calc-alkaline suite			Mildly alkaline suite		
	step 1	*step 2*	*step 3*	*step 1*	*step 2*	*step 3*
A. Initial melt compositions						
wt%	BA	A	Rd	BTa	Ta	LSR
SiO_2	54.17	58.72	70.17	51.73	60.26	73.31
TiO_2	1.21	0.92	0.52	2.59	1.37	0.14
Al_2O_3	17.27	17.36	16.34	16.66	16.15	13.77
Fe_2O_3*	8.78	3.85	3.06	12.28	7.52	2.35
MnO	0.10	0.82	0.04	0.13	0.10	0.01
MgO	4.79	2.25	0.91	3.54	2.39	0.51
CaO	8.80	8.70	0.96	5.97	4.17	0.36
Na_2O	3.89	5.81	4.26	3.73	3.95	2.35
K_2O	0.82	1.35	3.59	2.50	3.56	7.17
P_2O_5	0.16	0.22	0.15	0.87	0.52	0.03
ppm						
Zr	127	136	162.7	416.6	515	283.4
Ce	38	43	57.7	124.4	158	164.8
Nb	6	7	11.7	41.5	36	27
V	183	72	39	158	92	5.4
B. Fractionating mineral assemblages, wt%						
Ol	10	-	-	32	-	-
Pig	-	-	-	-	18	-
Aug	24	32	-	-	9.5	-
Hbl	-	-	22	-	-	-
Bt	-	-	15	-	-	-
Pl	53	57	55	52	60	30
Kfs	-	-	-	-	-	62
Sp	10	8	6	7	6	6
Ilm	2.5	2	0.40	7	4	0.80
Ap	-	0.70	1.2	2	2.5	0.50
Zrn	0.01	0.01	0.08	0.01	0.02	0.06
All	-	-	-	-	-	0.30
C. Composition of fractionating phases						
Ol	Fo50	-	-	Fo40	-	-
Pig	-	-	-	-	528	-
Aug	145	145	-	-	145	-
Hbl	-	-	143	-	-	-
Bt	-	-	628	-	-	-
Pl	An50	An50	An50	An80	An50	An30
Kfs	-	-	-	-	-	Or85
Sp	501	501	615	781	647	680
Ilm	*ideal*	*ideal*	*ideal*	784	410	410
Ap	-	*ideal*	*ideal*	*ideal*	*ideal*	*ideal*

Numbers refer to the chemical analyses of minerals in Tables 2 (for Pig, Aug and Hbl), 3 (for Bt) and 4 (for Sp and Ilm). Ideal compositions with a given Fo, An and Or content were used for Ol, Pl and Kfs, and ideal compositions of pure phases were also used for Ap and some Ilm

D. Mineral-melt partition coefficients
(from Rollinson, 1993)

step 1	Zr	Nb	Ce	V
Ol	0.012	0.01	0.006	0.06
Cpx	0.1	0.005	0.092	1.35
Pl	0.048	0.01	0.111	
Sp	0.1	0.4	2.1	26
Ilm		20*	1.64*	
Ap	0.1*	0.1*	21.1*	
Zrn	4700*	50*	4.31*	

step 2	Zr	Nb	Ce	V
Cpx	0.162	0.3	0.084	1.1
Pl	0.013	0.025	0.136	0.01
Sp	0.2	1	0.2	30
Ilm		20*	1.64*	
Ap	0.1*	0.1*	21.1*	
Zrn	4700*	50*	4.31*	

step 3	Zr	Nb	Ce	V
Cpx	0.6	0.8	0.5	
Hbl	4	4	1.52	30*
Bt	1.2	6.37	4.36	30*
Pl	0.135	0.06	0.267	
Kfs	0.03	0.01*	0.037	
Sp	0.8	2.5		35*
Ilm		20*	1.64	
Ap	0.1	0.1	21.1	
Zrn	4700*	50*	4.31	
All	1*	3*	635	

* – arbitrary values

PALAEOGEOTECTONIC SIGNIFICANCE OF THE GEOCHEMICAL VARIATION OF THE VOLCANIC ROCKS

The Carboniferous–Permian volcanism in the Intra-Sudetic Basin clearly represented late to post-collisional activity, associated with extension in the eastern part of the Variscan orogen of Europe. Therefore the geochemical variation of the volcanic rocks with time, from calc-alkaline, convergent plate margin-like (in the early and

late Carbonifeorus), to mildly alkaline, largely within-plate (in the late Carboniferous and early Permian), cannot be interpreted as a direct effect of a changing geodynamic regime from a convergent plate margin to a within-plate setting. Furthermore, calc-alkaline volcanic rocks with convergent plate margin geochemical signatures are not uniquely associated with contemporaneous subduction at convergent plate boundaries. Such volcanic rocks also erupt in post-collisional, extensional settings adjacent to former active continental margins (e.g. the Basin and Range province of the SW USA), especially during the first 10–20 Ma after the collision (Desonie, 1992; Davies *et al.*, 1993; Davies & Hawkesworth, 1995; Pouclet *et al.*, 1995; Wang *et al.*, 1999), often with a later switch towards alkaline volcanism (Davies *et al.*, 1993; Pouclet *et al.*, 1995). It is thus possible that the geochemistry of the older, calc-alkaline suite of the Intra-Sudetic Basin represented an "echo" of subduction processes that possibly preceded the Variscan collision and orogeny, while the younger, mildly alkaline suite, represented a transition towards post-orogenic, intracontinental, rift-related volcanism.

DISCUSSION

The major element geochemistry and origin of the volcanic rocks of the Intra-Sudetic Basin were previously considered by Nowakowski (1968), Pendias and Ryka (1978), Lis and Sylwestrzak (1980), Ryka (1989) and Wierzchołowski (1993). The volcanic rocks were variously classified as tholeiitic (Pendias and Ryka) or calc-alkaline (Nowakowski, Wierzchołowski). It was generally suggested that the basic/intermediate volcanic rocks originated due to crustal contamination (or mixing with crustal magmas) of mantle-derived melts, while the acidic volcanic were largely anatectic crustal magmas. These results, however, must be considered preliminary and speculative because of the limited evidence.

Problems of the major and trace element geochemistry and petrogenesis of the volcanic rocks of the Intra-Sudetic Basin were recently addressed in several papers published by Dziedzic (1996, 1998, and references therein). The key conclusions of these studies may be summarised as follows: 1) the volcanic activity in the Intra-Sudetic Basin occurred in Permian times, 2) the volcanic rocks represent a bimodal suite, with subordinate calc-alkaline and picritic varieties emplaced prior to the dominant "subtholeiitic" rocks, 3) the volcanic rocks originated from garnet-bearing, asthenospheric mantle sources, with partial melting degrees increasing (?with time) from the calc-alkaline through the picritic to the "subtholeiitic" series, 4) the latter series underwent extensive assimilation-fractional crystallisation processes within the lower crust, 5) the acidic rocks originated from the associated less evolved magmas due to both closed-system fractional crystallisation and assimilation-fractional crystallisation within the upper crust, 6) the volcanism occurred in a rift zone ("...the Silesian Rift considered as part of the Early Devonian rift zone in Central Europe"; Dziedzic, 1998, p. 90).

Most of these conclusions substantially differ from the results reported in this paper. The main differences refer to the age of the volcanic activity, the classification of the volcanic rocks and volcanic rock suites, the origin and differentiation of magmas and the geodynamic setting of the volcanic activity. This possibly largely results from a more general approach to both geology and geochemistry applied in the papers discussed.

CONCLUSION

The Carbonifeorus–Permian volcanic rocks of the Intra-Sudetic Basin represent products of late- to post-collisional volcanism associated with extension within the eastern part of the Variscan belt of Europe. Based on the geology and geochemistry the volcanic succession is subdivided into two suites: the older suite, erupted in the early and late Carboniferous, and the younger suite, erupted in the late Carboniferous and early Permian. The older suite consists of rhyodacites with subordinate basaltic andesites and andesites. These rocks show calc-alkaline, convergent plate margin-like affinities. The younger suite consists of rhyolitic tuffs, rhyolites and less widespread trachyandesites and basaltic trachyandesites. They are characterised by mildly alkaline and within-plate affinities, with some gradations towards convergent-plate margin lavas. This geochemical variation compares well with that found in some Tertiary–Recent post-collisional, extensional settings adjacent to former active continental margins (e.g. the Basin and Range province of the SW USA).

The parental magmas for each suite possibly originated from similar, garnet-free mantle sources at relatively shallow depths (within the subcontinental mantle?), but at variable degrees of partial melting (lower for the mildly alkaline rocks). The convergent plate margin-like geochemical signatures of the volcanic rocks may either have been inherited from their mantle sources, or be related to the assimilation of crustal rocks by the ascending and fractionating primary magmas. The major and trace element variation in both suites can largely be modelled as a closed

system fractional crystallisation. Different mineral assemblages, equivalent to the observed phenocrysts, fractionated from the magmas in each suite. Plagioclase and pyroxene, along with hydrous phases (hornblende, biotite) at the late stages of differentiation, fractionated from the calc-alkaline magmas. The fractionating assemblages in the mildly alkaline suite changed from plagioclase-dominated, with olivine and pyroxenes. to K-feldspar-dominated, with less abundant plagioclase. Accessory Fe-Ti oxides, apatite and zircon accompanied the major minerals in both suites, and the trace element patterns of the acidic mildly alkaline rocks were also strongly influenced by fractionation of other accessory minerals (? monazite, ? xenotime). In addition, the petrographic evidence (e.g. quartz phenocrysts with reaction rims, complexly zoned or sieve-textured feldspar phenocrysts) suggests that assimilation and/or magma mixing processes might also have taken place during the evolution of the magmas.

Acknowledgements

I wish to thank Prof. Ryszard Kryza and Prof. Malcolm Howells for their critical comments on the early versions of the paper and helpful discussions on the problems of volcanology, petrology and geochemistry. I am grateful to Henryk Siaglo, MSc., and Janusz Rzechonek for the preparation of thin sections. The financial support for this research was provided by the University of Wroclaw (grants 2093/W/ING/91, 2022/W/ING/92/17, 2022/W/ING/94-18, 2093/W/ING/93-2, 1017/S/ING/92-96-II) and MEN (grant P/02/032). The analytical work (XRF and microprobe) was mainly carried out at the British Geological Survey, Keyworth, UK, and also at the Université Blaise Pascal, Clermont-Ferrand, France, and at Keele University, UK. The British Council funded the fellowship at the BGS; the fellowship at the UBP was funded from the Polish-French Joint Project (ATP 10 6090), and the fellowship at Keele University from Tempus JEP No. 3656. All these institutions, their managers and staffs are gratefully acknowledged.

REFERENCES

AWDANKIEWICZ, M., 1997 a. Permski wulkanizm bazaltowy w środkowej części niecki śródsudeckiej. [Permian basaltic volcanism in the central part of the Intra-Sudetic Basin, SW Poland]. *Acta Universitatis Wratislaviensis No 1917, Prace geologiczno-mineralogiczne*, LV: 43–70.

AWDANKIEWICZ, M., 1997 b. *Petrology and geochemistry of the Carboniferous and Permian volcanic rocks of northern part of the Intra-Sudetic Basin, SW Poland.* Biblioteka Instytutu Nauk Geologicznych Uniwersytetu Wroclawskiego, 175 p. (unpublished).

AWDANKIEWICZ, M., 1999. Volcanism in a late Variscan intramontane trough: Carboniferous and Permian volcanic centres of the Intra-Sudetic Basin, SW Poland. *Geologia Sudetica,* 32: 13–47.

BENEK, R., KRAMER, W., McCANN, T., SCHECK, M., NEGENDANK, J. F. W., KORICH, D., HUEBSHER, H.-D. & BAYER, U., 1996. Permo-Carboniferous magmatism of the Northeast German Basin. *Tectonophysics,* 266: 379–404.

COX, K. G., BELL, J. D. & PANKHURST, R. J., 1979. *The interpretation of igneous rocks.* George Allen and Unwin, London, 450 p.

DAVIS, J.M., ELSTON, W.E. & HAWKESWORTH, C. J., 1993. Basic and intermediate volcanism in the Mogollon-Datail volcanic field: implications for mid-Tertiary tectonic transitions in southwestern New Mexico, USA. In: Prichard H.M., Alabaster T., Harris N.B.W. & Neary C.R. (eds.): Magmatic Processes and Plate Tectonics. *Geological Society Special Publication*, 76: 469–488.

DAVIS, J. M. & HAWKESWORTH, C. J., 1995. Geochemical and tectonic transitions in the evolution of the Mogollon-Datail Volcanic Field, New Mexico, U.S.A. *Chemical Geology*, 119: 31–53.

DESONIE, D. L., 1992. Geologic and geochemical reconnaissance of Isla San Esteban: post-subduction orogenic volcanism in the Gulf of California. *Journal of Volcanology and Geothermal Research*, 52: 123–140.

DZIEDZIC, K., 1996. Two-stage origin of the Hercynian volcanics in the Sudetes, SW Poland. *Neues Jahrbuch für Mineralogie, Geologie und Palaeontologie,* 199: 65–87.

DZIEDZIC, K., 1996. Genesis and evolution of Sudetic late Hercynian volcanic rocks inferred from trace element modelling. *Geologia Sudetica,* 31: 79–91.

HEY, M. H., 1954. A new review of the chlorites. *Mineralogical Magazine,* 30: 277–92.

HOWELLS, M., REEDMAN, A. J. & CAMPBELL, D. G., 1991. *Ordovician (Caradoc) marginal basin volcanism in Snowdonia (north-west Wales).* London, HMSO for the British Geological Survey, 191 p.

KUNO, H., 1966. Lateral variation of basalt magma types across continental margins and island arcs. *Bulletin Volcanologique,* 29: 195–222.

LE MAITRE, R. W., BATEMAN, P., DUDEK, A., KELLER, J., LAMEYRE, J., LE BAS, M. J., SABINE, P. A., SCHMID, R., SORENSEN, H., STRECKEISEN, A., WOOLEY, A. R. & ZANETTIN, B., 1989. *A classification of igneous rocks and glossary of terms. Recommendations of the International Union of Geological Sciences Subcomission on the Systematics of Igneous Rocks.* Blackwell, Oxford, 193 p.

LEAT, P. T., JACKSON, S. E., THORPE, R. S. & STILLMAN, C. J., 1986. Geochemistry of bimodal basalt-subalkaline/peralkaline rhyolite provinces within the Southern British Caledonides. *Journal of the Geological Society, London,* 143: 259–273.

LIS, J. & SYLWESTRZAK, H., 1980. Petrochemiczne zróżnicowanie a geneza mlodopaleozoicznych wulkanitów Dolnego Śląska [Petrochemical differentiation and genesis of young Palaeozoic volcanites in Lower Silesia]. *Przegląd Geologiczny,* 80: 92–98.

LORENZ, V. & NICHOLLS, I. A., 1976. The Permocarboniferous basin and range province of Europe. An application of plate tectonics. In: Falke, H. (Ed.): *The continental Permian in Central, West and South Europe.* Dordrecht, pp. 313–342.

LORENZ, V. & NICHOLLS, I. A., 1984. Plate and intraplate processes of Hercynian Europe during the Late Paleozoic. *Tectonophysics,* 107: 25–56.

NOWAKOWSKI, A., 1968. Wulkanity permskie Gór Suchych w niecce śródsudeckiej. [Permian volcanites of the Suche Mts. in the Intra-Sudetic Basin]. *Geologia Sudetica,* 4: 299–

408.

PEARCE, J. A. 1983. Role of the subcontinental lithosphere in magma genesis at active continental margins. In: Hawkesworth C. J. & Norry M. J. (eds.): *Continental basalts and mantle xenoliths*. Shiva, Nantwich, 230–249.

PEARCE, J. A., HARRIS, N. B. W. & TINDLE, A. G., 1984. Trace Element Discrimination Diagrams for the Tectonic Interpretation of Granitic rocks. *Journal of Petrology*, 25: 956–983.

PENDIAS, H. & RYKA, W., 1978. Subsequent Variscan volcanism in Poland. *Zeitschrift fuer Geologische Wissenschaften*, 6: 1081–1092.

POUCLET, A., LEE, J. S., VIDAL, P., COUSENS, B. & BELLON, H., 1995. Cretaceous to Cenozoic volcanism in South Korea and in the Sea of Japan: magmatic constraints on the opening of the back arc basin. In: Smellie J. L. (ed.): Volcanism Associated with Extension at Consuming Plate Margins. *Geological Society Special Publication*, 81: 77–93.

ROLLINSON, H. R., 1993. *Using Geochemical Data: Evaluation, Presentation, Interpretation.* Longman Scientific & Technical, 352 pp.

RYKA, W., 1989. Rotliegendes Volcanics, Sediment Lithologies and Paleoenvironments, and Polish Basin History: An Overview. In: Boyle, R. W. Brown, A. C. Jefferson, C. W. Jowett, E. C. and Kirkham, R. V. (eds.): Sediment-hosted Stratiform Copper Deposits. *Geological Association of Canada Special Paper* 36: 627–633.

WANG, K. L., CHUNG, S.-L., CHEN, C.-H., SHINJO, R., YANG, T. F. & CHEN, C.-H., 1999. Post-collisional magmatism around northern Taiwan and its relation with opening of the Okinawa Trough. *Tectonophysics*, 308: 363–376.

WIERZCHOLOWSKI, B., 1993. Pozycja systematyczna i geneza sudeckich skał wulkanicznych. [Systematic position and genesis of the Sudetic volcanic rocks]. *Archiwum Mineralogiczne*, 49: 199–235

WILSON, M., 1989. *Igneous Petrogenesis.* Harper Collins Academic, 466 p.

WINCHESTER, J. A. & FLOYD, P. A., 1977. Geochemical discrimination of different magma series and their differentiation products using immobile elements. *Chemical Geology*, 20: 325–343.